

AWARD NUMBER: **W81XWH-14-1-0094**

TITLE: "Defects in Histone H3.3 Phosphorylation and ATRX Recruitment to Misaligned Chromosomes during Mitosis Contribute to the Development of Pediatric Glioblastomas

PRINCIPAL INVESTIGATOR: Edward H. Hinchcliffe, Ph.D.

CONTRACTING ORGANIZATION: University of Minnesota, Twin Cities
Minneapolis, MN 55455

REPORT DATE: September 2015

TYPE OF REPORT: Annual

PREPARED FOR: U.S. Army Medical Research and Materiel Command
Fort Detrick, Maryland 21702-5012

DISTRIBUTION STATEMENT: Approved for Public Release;
Distribution Unlimited

The views, opinions and/or findings contained in this report are those of the author(s) and should not be construed as an official Department of the Army position, policy or decision unless so designated by other documentation.

REPORT DOCUMENTATION PAGE			<i>Form Approved</i> <i>OMB No. 0704-0188</i>	
Public reporting burden for this collection of information is estimated to average 1 hour per response, including the time for reviewing instructions, searching existing data sources, gathering and maintaining the data needed, and completing and reviewing this collection of information. Send comments regarding this burden estimate or any other aspect of this collection of information, including suggestions for reducing this burden to Department of Defense, Washington Headquarters Services, Directorate for Information Operations and Reports (0704-0188), 1215 Jefferson Davis Highway, Suite 1204, Arlington, VA 22202-4302. Respondents should be aware that notwithstanding any other provision of law, no person shall be subject to any penalty for failing to comply with a collection of information if it does not display a currently valid OMB control number. PLEASE DO NOT RETURN YOUR FORM TO THE ABOVE ADDRESS.				
1. REPORT DATE September 2015		2. REPORT TYPE Annual		3. DATES COVERED 1 Sep 2014 - 31 Aug 2015
4. TITLE AND SUBTITLE Defects in Histone H3.3 Phosphorylation and ATRX Recruitment to Misaligned Chromosomes during Mitosis Contribute to the Development of Pediatric Glioblastomas			5a. CONTRACT NUMBER	
6. AUTHOR(S) Edward H. Hinchcliffe, Ph.D. E-Mail: ehinchcliffe@hi.umn.edu			5b. GRANT NUMBER W81XWH-14-1-0094	
7. PERFORMING ORGANIZATION NAME(S) AND ADDRESS(ES) Hormel Institute, University of Minnesota, 801 16 th Ave NE Austin, MN 55912 801			5c. PROGRAM ELEMENT NUMBER	
			5d. PROJECT NUMBER	
9. SPONSORING / MONITORING AGENCY NAME(S) AND ADDRESS(ES) U.S. Army Medical Research and Materiel Command Fort Detrick, Maryland 21702-5012			5e. TASK NUMBER	
			5f. WORK UNIT NUMBER	
			8. PERFORMING ORGANIZATION REPORT NUMBER	
12. DISTRIBUTION / AVAILABILITY STATEMENT Approved for public release; distribution unlimited			11. SPONSOR/MONITOR'S REPORT NUMBER(S)	
13. SUPPLEMENTARY NOTES				
14. ABSTRACT Here we identify a conserved feedback mechanism that monitors the relative position of lagging chromosomes during anaphase via the differential phosphorylation of the histone variant H3.3 at Ser31. We examined non-transformed cells induced to missegregate chromosomes by transiently depolymerizing spindle microtubules with cold. After re-warming, correlative same cell live and fixed imaging revealed that isolated chromosomes (e.g. lagging in anaphase) have hyper-phosphorylated H3.3 Ser31 (pS31) along their arms that persists into G1. Surprisingly, during telophase Ser31 phosphorylation along individual chromosomes initiates global phosphorylation of H3.3 Ser31 in both reforming nuclei, suggesting an explanation for why both daughter cells trigger p53 activation in response to a single chromosome missegregation event. pS31 is mimicked by the localization of ATRX to isolated chromosomes. ATRX - a member of the SWI/SNF family of chromatin binding protein. We demonstrate that post-anaphase H3.3 pS31 and ATRX are required to trigger p53 stabilization in the subsequent G1 by microinjection of monospecific antibodies against either pS31 or ATRX into anaphase cells containing lagging chromosomes. This blocks p53 accumulation in G1 nuclei. In summary, we show that p53 cell cycle arrest - triggered by chromosome missegregation - is mediated via a novel signaling mechanism dependent upon H3.3 S31 phosphorylation and ATRX recruitment to lagging chromosomes. This work provides insight into how aneuploidy is normally monitored and suppressed.				
15. SUBJECT TERMS Aneuploidy/histone H3.3 Ser31 phosphorylation/ATRX mutation/antibody microinjection/p53 Somatic mutation/				
16. SECURITY CLASSIFICATION OF:				
a. REPORT Unclassified				
			17. LIMITATION OF ABSTRACT UU	18. NUMBER OF PAGES 43
			19a. NAME OF RESPONSIBLE PERSON USAMRMC	
			19b. TELEPHONE NUMBER (include area code)	

Standard Form 298 (Rev. 8-98)
Prescribed by ANSI Std. Z39.18

Table of Contents

	<u>Page</u>
1. Introduction.....	4
2. Keywords.....	4
3. Accomplishments.....	4
4. Impact.....	9
5. Changes/Problems.....	10
6. Products.....	10
7. Participants & Other Collaborating Organizations.....	11
8. Special Reporting Requirements.....	12
9. Appendices.....	12

1. Introduction: For persons under the age of 20, primary brain tumors are the leading cause of cancer-related mortality. For those aged 20-39 these tumors are the third-leading cause. Among these cancers, high-grade gliomas (HGGs), including glioblastoma multiform (GBM) and diffuse intrinsic pontine glioma (DIPG) arise de novo. These tumors appear distinct from adult glial-cell cancers. Pediatric cancers of the brain inordinately affect military service members and their families, with devastating effects on the military community, and increased cost for military health care services. To better understand the genetic alterations underlying the progression of pediatric brain cancers, independent studies utilized direct exome sequencing of tumor samples, and identified recurring somatic mutations leading to single amino acid substitutions in four genes: the p53 tumor suppressor, the histone variant H3.3, ATRX, and DAXX. As part of this project, we have shown that a residue on the N-terminal tail of histone H3.3 – Ser31 – is hyper phosphorylated in response to chromosome missegregation. We are characterizing this phosphorylation and the roles of ATRX and DAXX in monitoring chromosome missegregation and preventing the resulting aneuploidy. During the recent grant period we demonstrated a direct link between Ser31 phosphorylation and ATRX recruitment to missegregated chromosomes, and the ability of those chromosomes to trigger p53 activation, thereby down-regulating cell cycle progression in response to aneuploidy.

2. Keywords: aneuploidy, ATRX, cell cycle, chromosome missegregation, CRISPR/Cas9, DAXX, glioblastoma, histone H3.3, microinjection, mitosis, p53, site-directed mutagenesis.

3. Accomplishments:

a. What were the major goals of the project?

Major Task 1: Microinject anti-H3.3 Ser31 phospho-antibodies into BSC1 H2B-GFP cells

(Target date September, 2015: status: complete. Completion date: August 2015).

Major Task 2: Development of Histone H3.3 KDR cell lines

(Target date December, 2015: status: 75% complete).

Major Task 3: Live-cell analysis of H3.3 KDR cell lines

(Target date March, 2016: status: 35% complete).

Major Task 4: Microinjection of anti-ATRX and anti-DAXX antibodies

(Target date March, 2016: status: 50% complete).

b. What was accomplished under these goals?

Over the first year reporting period, we have had success in all of our major tasks. In our first task, we have completed the microinjection experiments using anti-phospho Ser31 and found that this masks the phosphorylation site *in vivo* and prevents the stabilization and activation of p53 in response to chromosome missegregation. This is a validation of our major hypothesis, that the mispositioning of chromosomes during mitosis can directly trigger p53 activation and cell cycle arrest, thereby preventing the proliferation of cells that inadvertently become aneuploid. We have also made headway on Task 2, the generation of knockdown/rescue cells, replacing WT histone H3.3 with mutant constructs. We have switched from shRNA hairpins to CRISPR/Cas9 gene editing to silence both alleles of H3.3 (and an H3.3-like gene found in the BSC1 genome). We have generated guide mRNAs and successfully transfected these into BSC1 cells. We have also generated point mutants in GFP-tagged H3.3 that either are non-phosphorylatable (S31A), constitutively phosphorylatable (S31E), or harbor the pediatric glioblastoma-linked driver mutations flanking the Ser31 site: K27M and G34R. We are analyzing the effects of their expression, as outlined in Task 3 of the application. Finally, we have begun the microinjection experiments described in Task 4 using antibodies against ATRX and DAXX. In our initial studies, we find that injecting anti-ATRX into anaphase cells induced to

have a lagging chromosome prevents p53 activation, reminiscent of the injection of anti-Ser31P antibodies. This strongly suggests that ATRX (mutated in pediatric glioblastoma patients) contributes to the genome proximity sensor effect, and resides in the same signaling pathway as phospho-H3.3. We have written our first manuscript from this work and submitted it to Nature Cell Biology. After favorable review, the manuscript was accepted with minor revision (i.e. the addition of a large number of control experiments). We have completed the revisions, and are submitting the revised manuscript in October of 2015. Below are detailed descriptions of the accomplishments made during the first grant period.

Task 1: Microinjection of anti-H3.3 Ser31 phospho-antibodies. To test whether there is a direct relationship between H3.3 Ser31P phosphorylation on missegregated chromosomes during anaphase and the subsequent activation of p53, we used microinjection of mono-specific anti-H3.3 Ser31P antibodies. For functional inactivation, direct needle antibody microinjection has a unique advantage over genetic manipulations (like siRNA) in that the injection can be precisely timed relative to a distinct cell cycle event (such as anaphase onset) on a time scale of minutes. This is particularly important here, given that we do not know the functional role of pericentromeric histone H3.3 Ser31 phosphorylation during normal mitosis. However, pericentromeric H3.3 Ser31 is normally dephosphorylated at anaphase onset, whereas the GPS signal monitoring chromosome missegregation triggers Ser31 phosphorylation during the anaphase/telophase transition. Thus, we use antibody microinjection to directly test whether H3.3 Ser31 phosphorylation, specifically associated with chromosome missegregation, can drive the stabilization and activation of p53 in an emerging aneuploid cell, overcoming any potential side effects of inhibiting pericentromeric Ser31P earlier in mitosis.

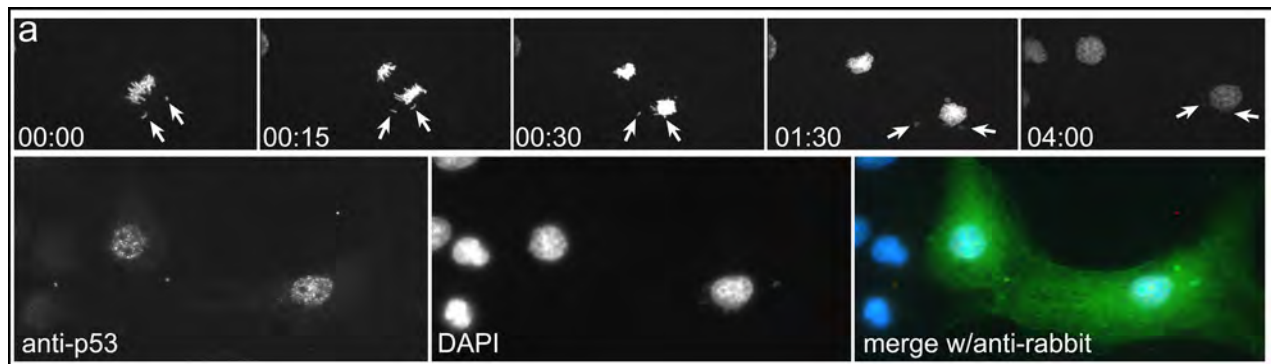


Figure 1. Microinjection of pre-immune IgG does not interfere with mitotic progression, but fails to inactivate p53 in response to chromosome missegregation. Top panels: frames from a time-lapse sequence showing a BSC1 cell induced to missegregate two chromosomes (arrows). Within 5 min of anaphase onset, the cell was injected with concentrated pre-immune rabbit IgGs. The cell was allowed to progress for ~4 hrs, then the coverslip removed from the chamber and fixed. The cell was labelled with mouse anti-p53 and counter-labelled with fluorescently tagged secondary antibodies against mouse (red) and rabbit (green) IgGs. In the bottom panels, the nuclei of the injected cell are positive for p53, indicating that the missegregation of chromosomes activated the aneuploidy fail-safe device. The two daughters are also positive for green anti-rabbit IgG, indicating that the microinjection was successful.

To control for the effects of microinjection, we injected concentrated pre-immune rabbit antiserum into re-warmed anaphase cells with a lagging chromosome (Figure 1). After fixation and labeling, these cells are easily identified because they contain rabbit IgGs detected by the addition of a fluorescent secondary antibody. Pre-immune antibodies did not prevent cells with lagging chromosomes from transitioning into interphase, or reforming nuclei. After 4 hrs, same cell fluorescence revealed that all control injected aneuploid cells accumulated nuclear p53 (N = 6), indicating that antibody injection does not inhibit the activation of the aneuploid fail-safe.

However, microinjection of concentrated anti-H3.3 Ser31P antibody into anaphase cells with lagging chromosomes (N = 11 cells) does not prevent reformation of daughter nuclei, but does block the activation of p53 in both daughter cells. This provides a direct biochemical link between chromosome missegregation (H3.3 Ser31 phosphorylation on lagging chromosomes) and triggering of the aneuploidy failsafe, which depends on the activation of p53.

The results of these experiments support our overall hypothesis, in which the so-called aneuploidy fail-safe, which triggers p53 activation and G₁ cell cycle arrest following chromosome missegregation during mitosis

occurs in direct response to the missegregation event, rather than in response to indirect effects, such as prolonged mitotic duration or DNA damage. Furthermore, these results reveal that the hyper-phosphorylation of histone H3.3 at position Ser31 along the arms of mispositioned chromosomes serves as the initial trigger for activation of the p53-dependant fail-safe. This strongly suggests the notion that the mutations observed in pediatric glioblastoma patients, which universally flank the Ser31 site, serve to down-regulate the ability of those cells to accurately monitor and respond to inadvertent chromosome missegregation. The resultant aneuploidy can conceivably play a role in the neoplastic progression of these nascent tumor cells.

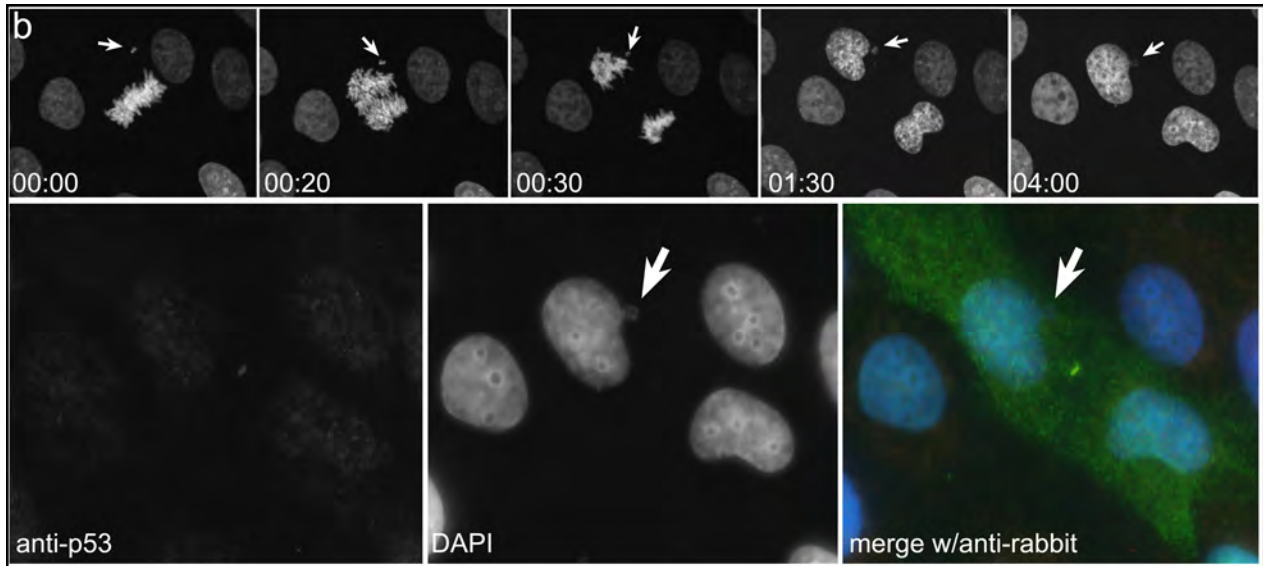


Figure 2. Microinjection of anti-Ser31P does not interfere with mitotic progression, but blocks the activation of p53 in response to chromosome missegregation. Top panels: frames from a time-lapse sequence showing a BSC1 cell induced to missegregate a single chromosome (arrow). Within 5 min of anaphase onset, the cell was injected with concentrated anti-Ser31P rabbit IgGs. The cell was allowed to progress for ~4 hrs, then the coverslip removed from the chamber and fixed. The cell was labelled with mouse anti-p53 and counter-labelled with fluorescently tagged secondary antibodies against mouse (red) and rabbit (green) IgGs. In the bottom panels, the nuclei of the injected cell are negative for p53, indicating that the activation the aneuploidy fail-safe device normally triggered by the missegregation of chromosomes has been blocked by the antibody. The two daughters are also positive for green anti-rabbit IgG, indicating that the microinjection was successful.

Task 2: Development of Histone H3.3 KDR cell lines. Green monkeys have 3 predicted genes for H3.3: H3F3A (GI: 103231004), H3F3B (GI: 103243033) and H3.3-like (103247374). We made 2 plasmids against H3F3B. Both plasmids had the Cas9 gene and a soluble GFP reporter. The CRISPR guide sequence in one of these plasmids was 100% match for the H3.3-like gene. Both guide sequences were 22 nucleotides long with the 100% match for H3F3B (and H3.3-like in one case). These guides were both 7 nucleotides different from any other known gene in the green monkey. We also made 2 plasmids against H3F3A. These had the cas9 gene and a soluble RFP reporter. Both guide sequences were 22 nucleotides long with 20 of those also matching the sequence for H3.3 like. Both sequences were 8 nucleotides different from any other known gene in the African green monkey genome. These were transfected into BSC1 cells. We identified multiple cells expressing both red and green reporter fluorescent proteins. However, no colonies formed, suggesting that loss of both histone H3.3 genes is lethal to cells.

While we were carrying out these experiments, a publication from another lab found that homozygous knockout of histone H3.3 in mice is embryonic lethal (Jang et al., 2015 Genes Dev. 29:1377-1392). So we switched strategies, and instead chose to generate cell lines expressing point mutants in GFP-tagged H3.3 genes that either are non-phosphorylatable (S31A), constitutively phosphorylatable (S31E), or harbor the pediatric glioblastoma-linked driver mutations flanking the Ser31 site: K27M and G34R. Interestingly, we found that all of these constructs act in a dominant-negative fashion, and induce chromosome instability (loss of chromosomes during cell division), via the generation of lagging chromosomes. This is not surprising; the mutations found in pediatric glioblastoma patients are heterozygous with a WT allele. Their actions would be predicted to serve as dominant.

Task 3: Live-cell analysis of H3.3 KDR cell lines. We are moving ahead with the characterization of the cells expressing point mutants in GFP-tagged H3.3 genes that either are non-phosphorylatable (S31A), constitutively phosphorylatable (S31E), or harbor the pediatric glioblastoma-linked driver mutations flanking the Ser31 site: K27M and G34R. As we cannot make permanent cells lines with these constructs (given that they induce chromosome segregation errors), we have turned to use of transient transfection and live-imaging within 36 hrs of expression. Analysis of live movies of cell division in cells expressing these mutants reveals defects in chromosome segregation, resulting in aneuploidy (Figs 3 and 4).

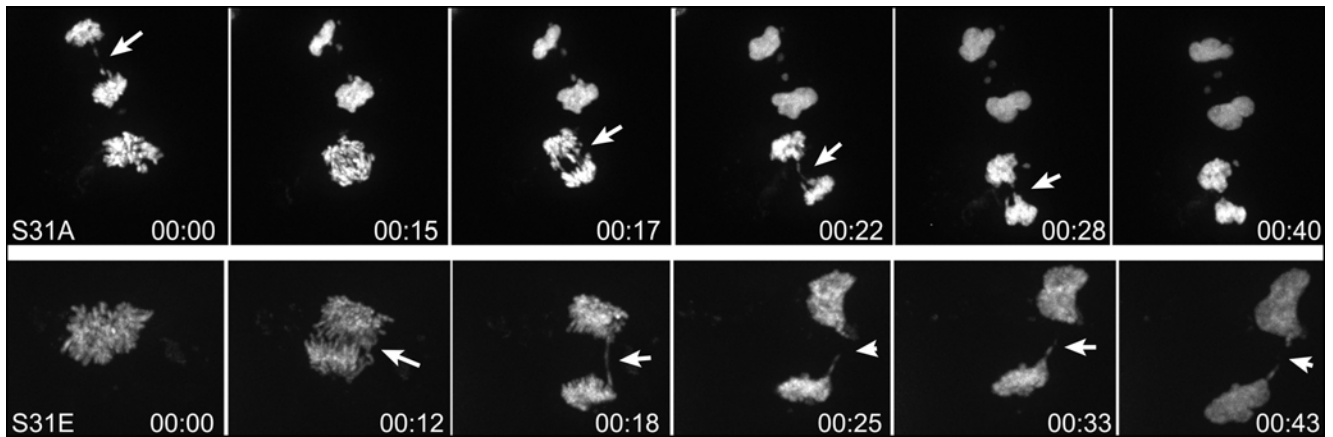


Figure 3. Expression of phosphorylation mutants of H3.3 Ser31 results in dominant negative chromosome segregation defects. Frames from time-lapse sequences of BSC1 cells transiently expressing GFP-fusion of histone H3.3 point mutants which induce single amino acid substitutions for position 31 (Ser). Top panels: S31A non-phosphorylatable mutant. Two cells showing chromosome segregation defects. The top cell is in anaphase, which chromosomes lagging in the central spindle region (arrow). The bottom cell progresses into anaphase and leaves a chromosome lagging, which forms a chromosome bridge (arrow). Bottom panels: S31E constitutively phosphorylated mutant. In this cell, a lagging chromosome bridge forms that persists as the cell reform their nuclear envelope (arrows). Time = hrs:min.

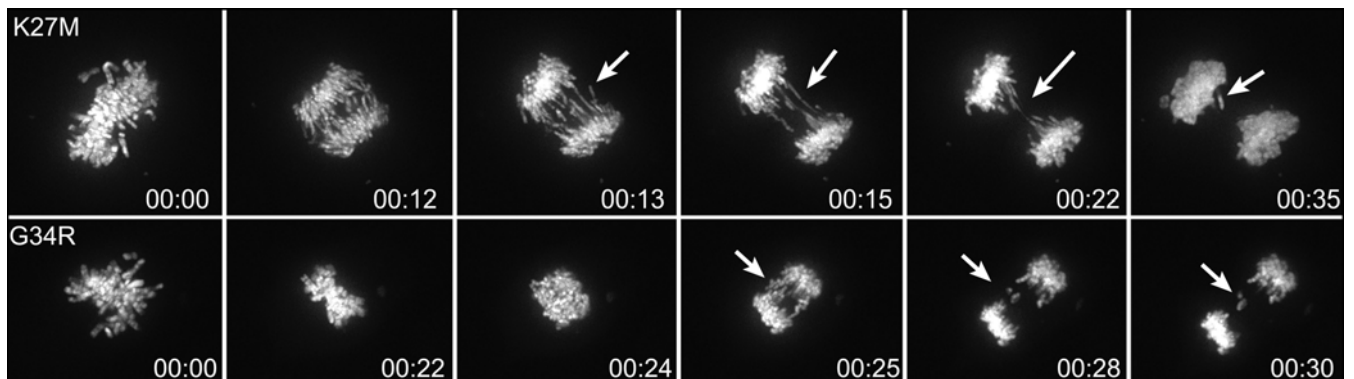


Figure 4. Expression of cancer-related mutants of H3.3 (flanking Ser31) results in dominant negative chromosome segregation defects. Frames from time-lapse sequences of BSC1 cells transiently expressing GFP-fusion of histone H3.3 point mutants which induce single amino acid substitutions for position 27 (Lys) and position 34 (Gly). Top panels: K27M cancer-associated mutant. The cell shows chromosome segregation defects. The cell progresses into anaphase and leaves a chromosome lagging, which forms a chromosome bridge (arrow). Bottom panels: G34R cancer-associated mutant. In this cell, a lagging chromosome persists during anaphase (arrows). Time = hrs:min.

We are continuing to generate data from these movies (increasing our numbers for analysis).

Task 4: Microinjection of anti-ATR_X and anti-DAXX antibodies.

α -thalassaemia/mental retardation X-linked (ATR_X) is a member of the SWI2/SNF2 family of helicase and ATPases, and has recently been shown to collaborate with DAXX to function as an H3.3 chaperone. ATR_X is also one of the proteins found mutated in pediatric glioblastomas. What makes this an important target for our experiments is the observation that anti-ATR_X antibodies decorate isolated chromosomes during both prometaphase and anaphase, similar to the pattern of H3.3 Ser31P seen as part of the GPS. To determine

whether ATRX on isolated chromosomes is required for the signalling of the p53-dependant aneuploidy fail-safe device, we used direct antibody microinjection. Cells were induced to missegregate chromosomes by chilling/rewarming, and as these entered anaphase, they were microinjected with concentrated anti-ATRX antibodies (Figure 5). After 4 hrs, the position of the microinjected cells were mark with a diamond scribe mounted in the nosepiece of the microscope, and the coverslip removed with the injection chamber and fixed in cold methanol. These cells lack nuclear p53 (which normally becomes stabilized and activated in response to chromosome missegregation). This strongly suggests that ATRX cooperates with the global H3.3 Ser31 phosphorylation along the arms of mislocalized chromosomes during anaphase.

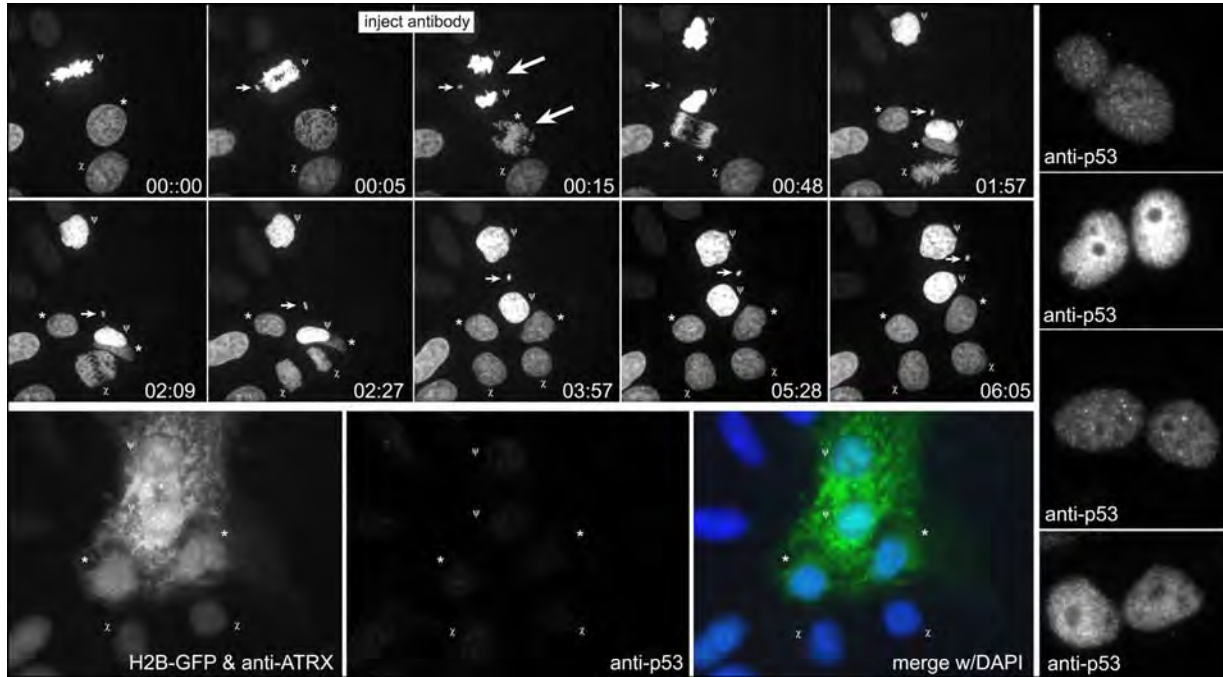


Figure 5. Microinjection of antibodies against ATRX prevents p53 activation in response to chromosome missegregation. Top panels show frames from a time-lapse sequence of three BSC1 cells, indicated by symbols (Ψ , \star , X). The Ψ cell, with a lagging chromosome (small arrow) divides first; while it is in anaphase, the \star cell is in prophase. (T = 5 min). At this time both cells were microinjected with concentrated anti-ATRX antibodies. These were then followed for 4 more hrs. During this time the X cell proceed through mitosis. At T = 06:05 there are three sets of daughter cells: the Ψ cells are aneuploid and microinjected; the \star cells are diploid and microinjected; the X cells are diploid and not microinjected. After scribing and fixation, the cells were labelled with anti-mouse p53, and secondary antibodies against mouse (red) and rabbit (green). There is no p53 in the nuclei of either the injected cells, regardless of whether they are aneuploid or diploid. As comparison, four tetraploid (binucleate) cells from the same coverslip were imaged with identical settings, showing the levels of nuclear p53 in these aneuploid cells. T = hrs:min.

c. What opportunities for training and professional development has the project provided?

"Nothing to Report."

d. How were the results disseminated to communities of interest?

In addition to the scientific presentations listed in the "PRODUCTS" section, Dr. Hinchcliffe has given several outreach presentations to local community and school groups during the past year.

Outreach presentation: given to PBS President Paula Kerger's visit to Hormel Institute.

Outreach presentation: given to Minnesota Chamber of Commerce Leadership Group, Austin, MN.

Outreach presentation: given to Austin Community Leadership Group, Austin, MN.

Outreach presentation: 7th grade class, Ellis Middle School (6x 1 hr presentations) Austin, MN.

e. What do you plan to do during the next reporting period to accomplish the goals?

Major Task 1: Microinject anti-H3.3 Ser31 phospho-antibodies into BSC1 H2B-GFP cells. For this task, the experiments are essentially done. We will complete this task by submitting our revised manuscript to Nature Cell Biology in October 2015.

Major Task 2: Development of Histone H3.3 KDR cell lines. For this task, our experiments are almost complete. We will confirm that the CRISPR/Cas9 silencing of the two BSC1 H3.3 genes is indeed lethal. We have switched to using the transiently transfected BSC1 cells expressing the GFP-coupled S31A, S31E, K27M and G34R mutants. These dominant negative heterozygous cells will be used to complete Task 3 below.

Major Task 3: Live-cell analysis of H3.3 KDR cell lines. We will use the cells generated in Task 2 to characterize the role of the GBM mutations and phosphorylation-deficient mutations in activating p53 in response to chromosome missegregation. We will use transfection, chilling/re-warming and live-cell imaging to complete this Task, following the proposed experiments as set out in the SOW.

Major Task 4: Microinjection of anti-ATRAX and anti-DAXX antibodies. We have begun the microinjection experiments using the ATRAX antibodies. During the next grant period we will complete these experiments and the associated controls. In addition, we will screen anti-DAXX antibodies, and prepare these for microinjection. Finally, we will generate the dominant-negative DAXX-GFP constructs and analyze these, using methods outlined in Task 3. We will complete this Task by preparing the ATRAX/DAXX work for publication in 2016.

4. IMPACT

a. What was the impact on the development of the principal discipline(s) of the project?

The major impact during this reporting period is the demonstration that microinjection of anti-H3.3 Ser31P antibodies mask the phosphorylation site in vivo and prevent the activation of p53 in response to chromosome missegregation. This experimental finding demonstrates that the H3.3 Ser31 phosphorylation in response to chromosome missegregation is one of the triggers responsible for inducing cell cycle arrest in reaction to aneuploidy. We have submitted the report of these findings to the journal Nature Cell Biology, and this work has been accepted for publication, pending minor revision.

The second major impact of our work is the discovery that mutations in the H3.3 gene (K27M and G34R) – found to be driver mutations in pediatric glioblastoma – cause defects in chromosome segregation when expressed. Therefore these function as dominant negatives. We also find the same result for expressing the non-phosphorylatable form of H3.3 (S31A mutant). This further suggests that the above mentioned cancer-causing mutations influence chromosome segregation and therefore chromosomal stability via modulations of the Ser31 phosphorylation site. Together, our results suggest that the GBM mutations induce a double hit: cause chromosome missegregation by potentially influencing Ser31 phosphorylation at the pericentromere, and then preventing the activation of the aneuploidy fail-safe, which recognizes chromosome segregation mistakes. The end result of these mutations would be the generation of aneuploid daughter cells which continue to proliferate. If our model is correct, this would imply that heterozygous mutations in this region of the H3.3 gene are particularly dangerous, and provides insights into how they drive cancer progression.

b. What was the impact on other disciplines?

"Nothing to Report."

c. What was the impact on technology transfer?

"Nothing to Report."

5. CHANGES/PROBLEMS:

a. Changes in approach and reasons for change

"Nothing to Report."

b. Actual or anticipated problems or delays and actions or plans to resolve them

"Nothing to Report."

c. Changes that had a significant impact on expenditures

Mr. Kul Karanjeet (our research technician) left the lab to take a position at the University of Minnesota School of Medicine. We hired Ms. Alyssa Langfald to replace him. There was a delay in identifying a suitable candidate and hiring her. She is now trained and fully engaged on the project. The laboratory also hired Dr. Charles Day as a post-doctoral fellow. Although originally hired to work on our NIH-funded project of phospholipases and sepsis, Dr. Day has switched full time to working on the DOD-funded glioblastoma project.

d. Significant changes in use or care of human subjects, vertebrate animals, biohazards, or agents

"Nothing to Report."

e. Significant changes in use or care of human subjects

"Nothing to Report."

f. Significant changes in use or care of vertebrate animals

"Nothing to Report."

g. Significant changes in use of biohazards and/or select agents

"Nothing to Report."

6. PRODUCTS:

a. Publications, conference papers, and presentations

Journal publications:

1. Hinchcliffe, E.H. (2015). "Video microscopy". *eLS*. DOI:10.1002/9780470015902. a0002638.
2. E H. Hinchcliffe, K.B. Karanjeet, C.A. Day, K.T. Vaughan, and Z. Dong. Histone H3.3 Ser31 phosphorylation on chromosomes lagging in anaphase triggers p53-dependant cell cycle arrest. *Nature Cell Biology*. 2015 (accepted with revision).

Books or other non-periodical, one-time publications

"Nothing to Report."

Other publications, conference papers, and presentations

- | | |
|-------|--|
| 09/15 | Speaker: <i>Minisymposium</i> , Chicago Cytoskeleton Meeting, Northwestern University, Chicago, IL. |
| 07/15 | Speaker: <i>Minisymposium</i> , 9 th Salk Institute Cell Cycle Meeting, Salk Institute, La Jolla, CA. |
| 06/15 | Speaker: <i>Minisymposium</i> , FASEB Science Research Conference: Mitosis: Spindle Assembly and Function. Big Sky, MT (work presented by post-doctoral fellow, Dr. Charles Day). |
| 04/15 | Speaker: <i>Minisymposium</i> , Oklahoma Medical Research Foundation, "Symposium 2015: Emerging Topics in Genome Stability", Oklahoma City, OK. |
| 04/15 | Invited seminar: Dept. Cell Biology, Univ. Massachusetts Medical School, Worcester, MA. |

b. Website(s) or other Internet site(s)

"Nothing to Report."

c. Technologies or techniques

"Nothing to Report."

d. Inventions, patent applications, and/or licenses

"Nothing to Report."

e. Other Products

"Nothing to Report."

7. PARTICIPANTS & OTHER COLLABORATING ORGANIZATIONS

What individuals have worked on the project?

Name:	Edward H. Hinchcliffe
Project Role:	PI
Person Months Worked:	6
Contribution to Project:	Cell biology and microinjection experiments
Funding Support:	NIH

Name:	Kul Karanjeet
Project Role:	Research Technician
Person Months Worked:	5
Contribution to Project:	Cell culture and molecular cloning
Funding Support:	NA

Name:	Charlie Day
Project Role:	Post-Doctoral Fellow
Person Months Worked:	6
Contribution to Project:	Molecular cloning, CRISPR, live-imaging
Funding Support:	NIH

Name:	Alyssa Langfald
Project Role:	Research Technician
Person Months Worked:	3
Contribution to Project:	Cell culture, molecular cloning
Funding Support:	NA

Has there been a change in the active other support of the PD/PI(s) or senior/key personnel since the last reporting period?

Our grant pending at the NIH (**R01HL125353-01**) was funded. There is no overlap between the aims of this NIH study and the present DOD grant.

1. **National Institutes of Health**, Research Grant R01HL125353-01. "The functional role of the cPLA2alpha/C1P interaction in sepsis resolution" 9/15/14 – 8/31/19. Role: PI

What other organizations were involved as partners?

"Nothing to Report."

8. SPECIAL REPORTING REQUIREMENTS

"Nothing to Report."

9. APPENDICES:

- a. Hinchcliffe et al., Nature Cell Biology manuscript (attached).

Histone H3.3 Ser31 phosphorylation on chromosomes lagging in anaphase triggers p53-dependant cell cycle arrest

Edward H. Hinchcliffe^{1*}, Kul B. Karanjeet¹, Charles A. Day¹,
Kevin T. Vaughan², and Zigang Dong^{1*}

¹Hormel Institute, University of Minnesota, Austin MN 55912 USA

²Department of Biological Sciences, University of Notre Dame,
Notre Dame IN, 46556 USA

*Authors for correspondence: ehinchcliffe@hi.umn.edu or zgdong@hi.umn.edu

Abstract

During mitosis the spindle assembly checkpoint (SAC) monitors bipolar kinetochore attachment to spindle microtubules, delaying anaphase onset until all chromatids are properly aligned^{1, 2}. However, maloriented kinetochore attachments can evade the SAC, leading to missegregated chromosomes and aneuploidy, a common feature of tumor cells^{3, 4}. Incidentally, chromosome missegregation in non-transformed cells triggers a p53-dependant cell cycle arrest in the ensuing G₁^{5, 6}. This acts as a fail-safe, blocking proliferation of normal cells that inadvertently become aneuploid. How this fail-safe is tripped is not known^{7, 8}. Here we identify a conserved feedback mechanism that monitors the relative position of lagging chromosomes during anaphase via the differential phosphorylation of histone H3.3 at Ser31⁹. We use chromosomally stable diploid cells, and induce transient chromosome missegregation by depolymerizing spindle microtubules with cold¹⁰. After re-warming, H3.3 Ser31 is phosphorylated exclusively at pericentromeres of all aligned chromosomes, which are rapidly dephosphorylated as they disjoin in anaphase. However, chromosomes lagging in anaphase accumulate H3.3 phospho-Ser31, spreading from the pericentromeres to chromosome arms. Remarkably, within minutes of anaphase onset Ser31 phosphorylation spreads from the single lagging chromosome to all the chromatids of both daughter cells and this phosphorylation persists into G₁. Next, we demonstrate that post-anaphase H3.3 phospho-Ser31 is directly required to trigger p53 stabilization. Masking H3.3 Ser31P by antibody microinjection into anaphase cells with lagging chromosomes prevents nuclear p53 accumulation in the aneuploid daughters. Previous work has shown that prolonged prometaphase can induce DNA damage, known to activate p53 stabilization¹¹⁻¹⁵. Here we show that chromosome missegregation can occur without prolonged mitotic duration, and that the activation of p53 occurs without DNA damage. Our discovery of this new signaling mechanism – termed the Genome Proximity Sensor (GPS) – provides insight into how aneuploidy, caused by maloriented chromosomes that slip past the SAC, is normally monitored and suppressed.

The interaction of mitotic spindle microtubules with the kinetochore region of sister chromatids functions to align chromatid pairs at the spindle equator². Microtubule-kinetochore interactions also recruit a positional sensing network (the SAC), which ensures bipolar chromosome alignment to the spindle. The kinetochore also monitors maloriented microtubule configurations, such as merotelic or syntelic attachments, and recruits proteins responsible for correcting these defects^{16, 17}. If left un-corrected, maloriented microtubule attachments can result in chromosomes lagging in anaphase, the “root cause of chromosome instability”⁴.

During mitosis the N-terminal tail of histone H3 is phosphorylated on multiple residues; these modifications modulate the binding of trans-acting proteins that alter chromatin structure, and regulate chromosome segregation¹⁸⁻²⁰. One poorly understood example of mitotic H3 phosphorylation occurs specifically on histone H3.3 at residue Ser31⁹. H3.3 is a histone variant replacing the canonical H3.1 via replication-independent deposition into core nucleosomes^{21, 22}. H3.3 differs from H3.1 by five highly conserved amino acid substitutions, including the A-31-S²². During normal mitosis H3.3 Ser31 is phosphorylated exclusively at pericentromeres, and is then rapidly dephosphorylated as sister chromatids disjoin in anaphase¹⁴. Despite being highly conserved, the role of H3.3 in chromatin architecture remains poorly understood, and at present the significance of mitotic H3.3 Ser31 phosphorylation at pericentromeres is not known.

We re-examined H3.3 Ser31 phosphorylation during mitosis, using a monospecific H3.3 phospho-Ser31 antibody and fluorescence microscopy (Fig. S1). Surprisingly, whereas H3.3 Ser31 phosphorylation is restricted to the pericentromeres of aligned chromosomes during prometaphase, on chromosomes that *misalign* (i.e. become isolated from the bulk of chromosomes congressing to the spindle equator) phospho-Ser31 spreads from the pericentromeres to the chromosome arms (Fig. 1). This suggests a previously uncharacterized gradient of H3.3 Ser31

phospho-activity in mitotic cells (Fig. S1). To accentuate the gradient, we used nocodazole treatment (2.5 μ M for 1 hr) to depolymerize spindle microtubules, allowing the mitotic chromosomes to partially disperse. Comparing fluorescence intensity levels of phospho-Ser31 on chromosome arms (not pericentromeres) revealed an average five-fold increase in phospho-Ser31 along misaligned arms (Fig. 1). Interestingly, the levels of Ser31-P on clustered chromosome arms decreases as a function of chromosome number suggesting a proximity effect (Fig. 1 and Fig. S1).

H3.3 Ser31 phosphorylation occurs along chromosomes that are misaligned, and therefore, have an active spindle assembly checkpoint (SAC). However, the Ser31 phosphorylation pattern does not mirror the SAC, which is activated by loss of microtubule attachment and tension across the centromeres². H3.3 Ser31 phosphorylation along the arms on an individual misaligned chromosome does not correlate with the proximity to spindle poles, or with absolute cellular position relative to the spindle equator (Fig. 1 and Fig. S1). The only factor that influences the levels of H3.3 Ser31P along chromosome arms is its lack of proximity to other chromosomes. We propose that this phosphorylation gradient is established by the aligned chromosomes, which induce dephosphorylation in *trans* to an individual chromosome as it aligns. This phosphorylation gradient serves as a biochemical proximity sensor monitoring chromosome misalignment; as a chromosome moves away from those congressing at the metaphase plate, it becomes phosphorylated. As a chromosome aligns at the spindle equator it is dephosphorylated (Fig. 1). We have termed this positional phospho-sensing mechanism the Genome Proximity Sensor (GPS).

The microtubule motor proteins cytoplasmic dynein/dynactin, CENP-E kinesin, and the chromokinesins are implicated in driving the congression of chromosomes to the spindle equator, and the genetic knockdown of chromokinesins causes abnormal chromosome arm orientation, delays in chromosome congression to the metaphase plate, and lagging chromosomes²³⁻²⁶. We

examined whether H3.3 Ser31P functions to recruit microtubule motor proteins to the arms of misaligned chromosomes (Fig. S2). However, fluorescence intensity measurements using antibodies against cytoplasmic dynein, the p150^{glued} subunit of dynactin, CENP-E, Hklp2, Kif4A and KID did not reveal an increase for misaligned vs aligned chromosome arms that correlates with the increase in H3.3 Ser31P levels (Fig. S2). Not surprisingly, the levels of dynein, p150^{glued} and CENP-E all substantially increase at the kinetochores of misaligned chromosomes (Fig. S2), as these function during congression and the remediation of the spindle assembly checkpoint^{25, 26}.

During abnormal mitosis, the loss/gain of a single chromosome by a normal diploid cell results in a G₁ cell cycle arrest in both the daughter cells, via the p53-dependant activation of the cyclin-dependent kinase inhibitor p21^{5-8, 27}. However, it is not known whether a single missegregated chromosome could directly signal the activation of p53⁸. To explore this, we developed a single-cell *In vivo* system, where chromosomally stable diploid cells undergo conditional chromosome instability during a single mitosis. We used normal BSC-1 (primate) cells expressing H2B-EGFP, as these remain relatively flat during mitosis and have wild-type p53^{28, 29}. To induce rapid, transient microtubule depolymerization we used chilling (4 °C for 20 min¹⁵); as the microtubules disassemble the mitotic chromosomes partially disperse. During the brief chilling, the spindle poles remain in place, so the overall geometry of the spindle axis does not change (Fig. 2). After re-warming to 37 °C, the spindle microtubules reform, the chromosomes align and the cells proceed through anaphase (Fig. 2). However, there is a significant increase in the frequency of chromosome missegregation events (Fig. 2). These arise from merotelic kinetochore attachments (kinetochore attached to microtubules emanating from both poles^{2, 4}), and/or syntelic kinetochore attachments (both kinetochores attached to microtubules emanating from a single pole¹⁶). The result is chromosomes lagging in the spindle midzone or spindle asters during anaphase (Fig. S3).

Following chilling/chromosome missegregation, both aneuploid daughter cells accumulate nuclear p53 (Fig. 2) and arrest in G₁ for ~60 hrs (Fig. S4). This arrest is not due to the cold treatment or imaging conditions, because control cells in the same field of view (subjected to identical cold treatment and imaging conditions) undergo repeated mitotic divisions (Fig. S4).

Prolonging prometaphase can also trigger p53 activation in the subsequent G₁¹⁰. To control for mitotic duration in our experiments, we measured the timing for cells that undergo the metaphase-anaphase transition while missegregating one or more chromosomes (Fig. 2). We find that on average, there is no significant difference in mitotic timing between cells that missegregate a chromosome (avg. 63 min, range 28-175 min), and those that do not (avg. 56 min, range 37-82 min). The few cells with prolonged prometaphase were excluded from further analysis of GPS.

To explore the role of GPS phospho-H3.3 signaling during chromosome missegregation, cells were chilled/re-warmed and individuals with lagging syntelic-attached chromosomes were followed by time-lapse spinning disk confocal microscopy as they progressed into anaphase. Within 2 min of anaphase onset, the position on the coverslip was marked with a diamond scribe in the nosepiece of the microscope²⁴, and the coverslip was fixed and labeled with anti-H3.3 Ser31P. Same-cell correlative live and fixed imaging revealed that the chromosomes lagging in anaphase have high levels of H3.3 Ser31 phosphorylation along their arms (N = 6), whereas regressing chromatid pairs that had properly aligned have ~10 fold less phosphorylation (Fig. 2).

This anaphase phospho-H3.3 pattern holds true for lagging chromosomes generated by merotelic attachments as well (N = 3). Unlike syntelic-attached chromosomes, merotelic-attached chromosomes align at the metaphase plate, and therefore, do not activate the GPS until after anaphase, when they separate from the regressing, disjointed sister chromatids (Fig. 2). Thus, the GPS signaling mechanism does not have to become activated prior to anaphase onset – it appears

that any chromosome that becomes isolated from the mass of chromosomes during mitosis can activate this proximity sensor. However, on occasion lagging chromosomes became “trapped” in the cleavage furrow (Fig. S3). Because of the potential for DNA damage, due to chromosome pulverization (known to activate p53^{7, 11}), we discarded these cells from further analysis.

Next we measured the time course for H3.3 Ser31 phosphorylation, beginning at anaphase disjunction, progressing through the time of nuclear envelope reformation in telophase, and ending at the stabilization of nuclear p53 in G₁. Unexpectedly we found that within 15 minutes of anaphase onset (a time well before the midbody assembles and the telophase daughter cells still share a common cytoplasm³⁰) both nascent daughter nuclei accumulate phospho-Ser31 (Fig. 3). H3.3 Ser31 phosphorylation persists in both daughter nuclei (and in the micronuclei formed by the missegregated chromosome) for ~3-4 hr post-anaphase, coincident with the time necessary to stabilize and activate p53^{6, 12, 31}. Importantly, the accumulation of H3.3 phospho-Ser31 in post-anaphase nuclei requires undergoing anaphase with a missegregated chromosome. If a lagging chromosome eventually aligns prior to anaphase onset (inactivating the GPS), then the levels of H3.3 Ser31P on the post-mitotic chromosomes decrease to baseline (N = 4; Fig. 3).

During prometaphase misaligned chromosomes activate the SAC, which monitors bipolar microtubule attachment to opposite kinetochores, and down-regulates cell cycle progression until all chromosomes are aligned^{2, 3}. However, because of the “rheostat nature” of the SAC, which under certain conditions allows cells with single mono-oriented chromosomes to transit the metaphase-anaphase transition, it is possible that these cells undergo anaphase with an active checkpoint³². To test this, individual mitotic cells with a syntelic-attached chromosome were followed by spinning disk confocal microscopy until they underwent anaphase. The coverslip was fixed within two minutes of anaphase onset, and labeled with antibodies against the SAC protein

BubR1. The kinetochore intensities of missegregated chromosomes in early anaphase were compared to kinetochore intensities of misaligned chromosomes in metaphase, where the checkpoint is known to be active (Fig. S5, N = 11 cells). BubR1 levels on syntelic chromosomes were greatly decreased in anaphase, strongly suggesting that these cells generate sufficient microtubule attachment and/or tension on the syntelic kinetochores to overcome the SAC^{16, 32}.

Cells that exit from prolonged mitosis (mitotic slippage) exhibit extensive DNA damage, which can be visualized as numerous phospho-H2AX foci^{7, 12-14}. We tested whether our cells, which exit mitosis with lagging chromosomes, but do not undergo prolonged mitosis, show evidence of DNA damage. Chromosome missegregation was induced by chilling/re-warming, and individual cells (N = 7) were followed by time-lapse microscopy as they entered G₁. After fixation and labeling with anti-phospho-H2AX, none of the aneuploid daughters showed phospho-H2AX foci (Fig. S5).

We further tested whether chromosome missegregation following chilling/re-warming induces p53 activation via the DNA damage pathway, using an inhibitor to the ATM kinase, which functions to transduce double stranded breaks into p53 activation³³. After chilling/re-warming, cells with syntelic chromosomes were followed until they underwent anaphase. Within two minutes of anaphase onset, the ATM inhibitor KU55933 (10 μ M) was added to the imaging chambers^{33, 34}. The cells were followed until 4 hrs post-anaphase, then fixed and labeled with anti-p53. All cells (N = 3) showed nuclear p53 accumulation in the absence of an effective ATM-mediated DNA damage response (Fig. S5). Together, these results suggest that the p53-dependant cell cycle arrest induced by the GPS occurs in direct response to chromosome missegregation, not via an indirect effect of abnormal mitosis, such as prolonged prometaphase or DNA damage.

To test whether there is a direct relationship between H3.3 Ser31P phosphorylation on missegregated chromosomes during anaphase and the subsequent activation of p53, we used

microinjection of mono-specific anti-H3.3 Ser31P antibodies. For functional inactivation, direct needle antibody microinjection has a unique advantage over genetic manipulations (like siRNA) in that the injection can be precisely timed relative to a distinct cell cycle event (such as anaphase onset) on a time scale of minutes. This is particularly important here, given that we do not know the functional role of pericentromeric histone H3.3 Ser31 phosphorylation during normal mitosis⁹. However, pericentromeric H3.3 Ser31 is normally dephosphorylated at anaphase onset, whereas the GPS signal monitoring chromosome missegregation triggers Ser31 phosphorylation during the anaphase/telophase transition. Thus, we use antibody microinjection to directly test whether H3.3 Ser31 phosphorylation, specifically associated with chromosome missegregation, can drive the stabilization and activation of p53 in an emerging aneuploid cell, overcoming any potential side effects of inhibiting pericentromeric Ser31P earlier in mitosis.

To control for the effects of microinjection, we injected concentrated pre-immune rabbit antiserum into re-warmed anaphase cells with a lagging chromosome. After fixation and labeling, these cells are easily identified because they contain rabbit IgGs detected by the addition of a fluorescent secondary antibody (Fig. 4). Pre-immune antibodies did not prevent cells with lagging chromosomes from transitioning into interphase, or reforming nuclei (Fig. 4). After 4 hrs, same cell fluorescence revealed that all control injected aneuploid cells accumulated nuclear p53 (N = 6), indicating that antibody injection does not inhibit the activation of the aneuploid fail-safe.

However, microinjection of concentrated anti-H3.3 Ser31P antibody into anaphase cells with lagging chromosomes (N = 11 cells) does not prevent reformation of daughter nuclei, but does block the activation of p53 in both daughter cells (Fig. 4). This provides a direct biochemical link between chromosome missegregation (H3.3 Ser31 phosphorylation on lagging chromosomes) and triggering of the aneuploidy failsafe, which depends on the activation of p53^{6, 8}.

In summary, we have demonstrated the existence of a novel signaling network that both monitors and suppresses the generation of aneuploidy in normal, diploid cells. This pathway utilizes a previously unrecognized histone phosphorylation gradient as a *Genome Proximity Sensor* (GPS). The sensor not only marks individual missegregated chromosomes, but also activates global H3.3 Ser31 phosphorylation of histones in both reforming nuclei, amplifying the signal in each daughter cell. We show that phospho-Ser31 in G₁ nuclei is required to initiate the p53 stabilization. Thus, the GPS acts as a direct switch that physically couples chromosome missegregation events with the induction of cell cycle arrest.

Our results are particularly interesting, given the recent findings of exome sequencing studies of pediatric glioblastoma multiform (GBM) patients, which uncovered recurring single nucleotide mutations in the H3.3 gene, but not in the H3.1 gene³³. Importantly these mutations result in amino acid substitutions in residues that flank Ser31 (K27M and G34R/G34V). Other mutations in GBM patients are found in the histone H3.3 binding proteins ATRX and DAXX²². ATRX is implicated in regulating mitotic chromosome dynamics³⁶ and DAXX is believed to modulate p53 stability via binding to MDM2³⁷. However, neither has been linked to H3.3 Ser31 phosphorylation.

The prevailing interpretations of these genetic studies suggest defects in epigenetic regulation underlie GBM pathogenesis. We suggest that defects in monitoring and suppressing aneuploidy may also play a role during tumorigenesis. Neuronal cells are known to become aneuploid, but this is not sufficient to drive tumorigenesis³⁸. However, the observed histone H3.3 somatic mutations may short-circuit the fail-safe, either by affecting phosphorylation in response to chromosome missegregation, or by changing the topology of the phospho-histone H3.3 so that it cannot recruit the factors necessary to activate p53 in response to chromosome missegregation. Either would allow cells that inadvertently become aneuploid to continue to proliferate.

Materials and methods

BSC-1 cells^{28,29} were transfected with histone H2B-GFP (Clontech, Mountain View, CA) and constitutively expressing cell lines selected as previously described²⁹. Cell lines were maintained at 37 °C and 10% CO₂ in Dulbecco's Modified Eagle Medium (DMEM: Sigma, St. Louis, MO).

Fixed cell immunofluorescence microscopy was performed as previously described³⁹. Briefly, BSC-1 cells were fixed in methanol at -20 °C, blocked in TBS (50 mM Tris, pH 7.4, 150 mM NaCl) 3% bovine serum albumin (BSA) and 0.5% Tween-20 for 1 hr at RT. Primary antibody incubations were diluted in 3% BSA/TBS for 16 hr at 4°C. Cells were washed three times for 10 min with 1% BSA/0.05% Tween TBS and incubated with 4', 6-diamidino-2-phenylindole (DAPI) diluted in TBS for 5 min. Coverslips were mounted using ProLong Gold anti-fade (Life Technologies, Carlsbad, CA). Primary antibodies and dilutions used are: anti-V3 dynein, 1:500 (ref 26); D'art, anti-p150, 1:500 (ref 26), anti-BubR1, 1:500 (BD, Franklin Lakes, NJ), anti-H2AX 1:2,000 and anti-p53, 1:1,000 (both Cell Signaling, Danvers, MA), anti-KID, 1:1,000, anti-KIF4, 1:1,000, anti-p53, 1:1,000 (all Santa Cruz Biotechnology, Santa Cruz, CA), anti-Aur A 1:1,000, and anti-histone H3.3 Ser31P, 1:5,000 (both AbCam, Cambridge, MA). Indirect fluorescence was achieved using Alexa 488, 594, or 660 conjugated secondary antibodies (Life Technologies).

Fixed cell images were collected using a Leica DM RXA2 microscope (Leica Microsystems, Buffalo Grove, IL), equipped with a 63x 1.4NA apo objective and Hamamatsu ORCA-ER CCD camera (Hamamatsu, Bridgewater, NJ). Images were collected as a Z-series, with 0.25 µm spacing. All images were exported to Adobe Photoshop (Adobe, San Jose, CA) for final layout.

The measurement of H3.3 phospho-Ser31 fluorescence levels on isolated chromosomes was done as described⁴⁰, modified here. Briefly, BSC-1 cells were plated on coverslips, then treated with 2.5 µM nocodazole for 1 hr. Cells were then immunolabelled with anti-H3.3 Ser31P and

anti-Aur A antibodies. Coverslips were scanned to identify cells with misaligned chromosomes, either single or clusters of two or more. A region of interest (ROI) was drawn over the chromosome arms, and three separate measurements per misaligned chromosome made and averaged together. Three ROIs of identical size away from the chromosomes to control for background were measured, averaged, and subtracted from the arm fluorescence. At least five cells for each condition were measured. Box and whiskers plots were made using Microsoft Excel.

For live-cell imaging, cells cultured on biocleaned coverslips were assembled into custom-built imaging chambers²⁹, filled with Phenol Red-free DMEM supplemented with 12.5 mM HEPES buffer. To transiently depolymerize spindle microtubules, imaging chambers were chilled to 4 °C for 20 min, then re-warmed to 37 °C on the live-cell imaging scope as previously described¹⁵.

Live-cell images were collected using a Yokogawa CSU-10 spinning disk confocal (Yokogawa Electric, Tokyo, Japan), with 200 mW 488nm diode laser (Coherent, Santa Clara, CA) and Hamamatsu 9100 EM-CCD camera mounted on a Leica DM RXA2 microscope equipped with a 63x 1.3NA glycerol immersion apo objective, housed in a custom-built plexiglas box and maintained at 37 °C with a proportional heat controller. All imaging systems were controlled by Simple PCI (Hamamatsu, Bridgewater, NJ) or Slidebook (3I, Denver CO) software. Time-lapse images were collected as a Z-series, with 2 μm spacing, with time intervals from one to five minutes between frames. Images are presented as maximum projections. The duration of prometaphase is defined here as the time interval between release of chromosomes from the disintegrating nuclear envelope until anaphase onset, as judged by sister chromatid disjunction.

Direct needle antibody microinjections were done using a Femtojet injector (Eppendorf, Hauppauge, NY) and MIS5000 piezo-electric micromanipulator (Burleigh/Thorlabs, Newton, NJ) on a Leica IRBE2 inverted microscope with a 40x 0.7NA objective and phase optics as previously

described²⁹. Briefly, pre-immune rabbit IgG or anti-H3.3 Ser31P rabbits antibodies were dialyzed into injection buffer (10 mM Na₂PO₄, pH 7.4, 100 mM KCl, 1 mM MgCl₂) overnight at 4 °C, then concentrated by centrifugation into a Amicon Ultra filter with a 50 kDa NMWL cutoff (EMD/Millipore, Billerica, MA). The concentrated antibody was centrifuged for 15 min at 15,000 rpm in an Eppendorf tabletop centrifuge just prior to use, and stored on ice until used. Microinjection needles were pulled from FHC 1.0 mm OD microcap tubes with microdot fiber (Frederick Haer Co, Bowdoinham, ME), using a Kopf vertical needle puller (David Kopf Instruments, Tujunga, CA). These needles were back-loaded with concentrated, cleared antibody using a Hamilton syringe (Hamilton Co, Reno, NV), and allowed to settle into the tip, aided by gentle flicking. Needles were used within 1 hr of loading. Chambers containing cells were chilled as described, then returned to the 37 °C spinning disk confocal, and scanned to identify a prometaphase cell with one or more syntellic, lagging chromosomes. These cells were followed by time-lapse imaging until anaphase onset (with a lagging chromosome) was observed. The position of the anaphase cell on the coverslip was marked with a circle etched by a diamond scribe mounted in the nosepiece of the microscope, then the chamber was transferred to the microinjection scope that had been pre-warmed with a commercial hair dryer (Vidal Sassoon, Santa Monica, CA). The needle was aligned, the tip broken on the edge of the coverslip, and the anaphase cell injected within five minutes of anaphase onset. The chamber was then returned to the confocal, and the injected cell followed by time-lapse microscopy for 4 hrs. The coverslip was then removed from the chamber, fixed and labelled with antibodies against p53 (mouse), and secondary anti-mouse (to detect the p53) and anti-rabbit (to identify the injected cell) were added. The position of the injected cell was determined using the diamond scribe mark, as viewed by a 10x 0.3 NA phase objective.

Acknowledgments

This work supported by the Hormel Foundation, Austin “Paint the Town Pink”, US Department of Defense (CDMRP) grant CA130436 and National Institutes of Health grant R01 HL125353 to EHH, and National Institutes of Health grant R01 CA166011 to ZD.

References

- 1. Dick, A.E., and D.W. Gerlich** (2013). Kinetic framework of spindle assembly checkpoint signalling. *Nat Cell Biol.* **15**:1370-1377.
- 2. London, N., and S. Biggins** (2014). Signalling dynamics in the spindle checkpoint response. *Nat Rev Cell Mol Biol.* **360**:553-68.
- 3. Bakhom, S.F., S.L. Thompson, A.L. Manning, and D.A. Compton** (2009). Genome stability is ensured by temporal control of kinetochore-microtubule dynamics. *Nat Cell Biol.* **11**:27–35.
- 4. Bakhom, S.F., W.T. Silkworth, I.K. Nardi, J.M. Nicholson, D.A. Compton, and D. Cimini** (2014). The mitotic origin of chromosomal instability. *Curr Biol.* **24**:R148-149.
- 5. Lanni, J.S., and T. Jacks** (1998). Characterization of the p53-dependent post-mitotic checkpoint following spindle disruption. *Mol Cell Biol.* **18**:1055-64.
- 6. Thompson, S.L., and D.A. Compton** (2010). Proliferation of aneuploid human cells is limited by a p53-dependent mechanism. *J Cell Biol.* **188**:369–381.
- 7. Ganem, N.J., and D. Pellman** (2012). Linking abnormal mitosis to the acquisition of DNA damage. *J Cell Biol.* **199**:871-881.
- 8. Hinchcliffe, E.H.** (2014). Centrosomes and the art of mitotic spindle maintenance. *Int Rev Cell Mol Biol.* **13**:179-218.
- 9. Hake, S.B., B.A. Garcia, M. Kauer, S.P. Baker, J. Shabanowitz, D.F. Hunt, and C.D. Allis** (2005). Serine 31 phosphorylation of histone variant H3.3 is specific to regions bordering centromeres in metaphase chromosomes. *Proc Natl Acad Sci USA* **102**:6344-6349.
- 10. Kasuboski, J.M., J.R. Bader, S.B.F. Tauhata, P.S. Vaughan, M. Winding, M.M. Morrissey, M.V. Joyce, W. Boggess, L. Vos, G.K. Chan, E.H. Hinchcliffe, and K.T. Vaughan** (2011). Zwint-1 is a novel Aurora B substrate required for the assembly of a dynein-binding platform on kinetochores. *Mol Biol Cell* **22**:3318-3330.
- 11. Rieder, C.L., and H. Maiato** (2004). Stuck in division or passing through: what happens when cells cannot satisfy the spindle assembly checkpoint. *Dev Cell* **7**:637-651.
- 12. Uetake, Y., and G. Sluder** (2010). Prolonged prometaphase blocks daughter cell proliferation despite normal completion of mitosis. *Curr Biol.* **20**:1666–1671.
- 13. Janssen, A., M. van der Burg, K. Szuhai, G.J.P.L. Kops, and R.H. Medema** (2011). Chromosome segregation errors as a cause of DNA damage and structural chromosome aberrations. *Science* **333**:1895-1898.

- 14. Hayashi, M.T., A.J. Cesare, J.A. Fitzpatrick, E. Lazzerini-Denchi, and J. Karlseder** (2012). A telomere-dependent DNA damage checkpoint induced by prolonged mitosis arrest. *Nat Struct Mol Biol.* **19**:387-394.
- 15. Crasta K., N.J. Ganem, R. Dagher, A.B. Lantermann, E.V. Ivanova, Y. Pan, L. Nezi, A. Protopopov, D. Chowdhury, and D. Pellman** (2012). DNA breaks and chromosome pulverization from errors in mitosis. *Nature* **482**:53–58.
- 16. Lončarek, J., O. Kisurina-Evgenieva, T. Vinogradova, P. Hergert, S. La Terra, T.M. Kapoor, and A. Khodjakov** (2007). The centromere geometry essential for keeping mitosis error free is controlled by spindle forces. *Nature* **450**:745-749.
- 17. Wang, F., N.P. Ulyanova, J.R. Daum, D. Patnaik, A.V. Kateneva, G.J. Gorbsky, and J.M. Higgins** (2012). Haspin inhibitors reveal centromeric functions of Aurora B in chromosome segregation. *J Cell Biol.* **199**:251-268.
- 18. Wang, F., J. Dai, J.R. Daum, E. Niedzialkowska, B. Banerjee, P.T. Stukenberg, G.J. Gorbsky, and J.M.G. Higgins** (2010). Histone H3 Thr-3 phosphorylation by haspin positions Aurora B at centromeres in mitosis. *Science* **330**:231-235.
- 19. Guse, A., C.W. Carroll, B. Moree, C.J. Fuller, and A.F. Straight** (2011). *In vitro* centromere and kinetochore assembly on defined chromatin templates. *Nature* **477**:354-358.
- 20. Fukagawa, T., and W.C. Earnshaw** (2014). The centromere: chromatin foundation for the kinetochore machinery. *Dev Cell.* **30**:496-508.
- 21. Tagami, H., D. Ray-Gallet, G. Almouzni, and Y. Nakatani** (2004). Histone H3.1 and H3.3 complexes mediate nucleosome assembly pathways dependent or independent of DNA synthesis. *Cell* **116**:51-61.
- 22. Elsässer, S.J. H. Huang, P.W. Lewis, J.W. Chin, C.D. Allis and D.J. Patel** (2012). DAXX envelops an H3.3–H4 dimer for H3.3-specific recognition. *Nature* **491**:560-565.
- 23. Kapoor, T.M., and D.A. Compton.** (2002). Searching for the middle ground: mechanisms of chromosome alignment during mitosis. *J Cell Biol.* **157**:551–556.
- 24. Wandke, C., M. Barisic, R. Sigl, V. Rauch, F. Wolf, A.C. Amaro, C.H. Tan, A. J. Pereira, U. Kutay, H. Maiato, P. Meraldi, and S. Geley** (2012). Human chromokinesins promote chromosome congression and spindle microtubule dynamics during mitosis. *J Cell Biol.* **198**:847-863.
- 25. Weaver, B.A.A., Z.Q. Bonday, F.R. Putkey, G.J.P.L. Kops, A.D. Silk, and D.W. Cleveland** (2003). Centromere-associated protein-E is essential for the mammalian mitotic checkpoint to prevent aneuploidy due to single chromosome loss. *J Cell Biol.* **162**:551–563.

- 26. Whyte J., J.R. Bader, S.B.F. Tauhata, M. Raycroft, J. Hornick, K.K. Pfister, W.S. Lane, G. Chan, E.H. Hinchcliffe, P.S. Vaughan, and K.T. Vaughan** (2008). Phosphorylation regulates targeting of cytoplasmic dynein to kinetochores during mitosis. *J Cell Biol.* **183**:819-834.
- 27. Pfau, S.J., and A. Amon** (2012). Chromosomal instability and aneuploidy in cancer: from yeast to man. *EMBO Reports* **13**:515–527.
- 28. Rigaudy, P., and W. Eckhart** (1989). Nucleotide sequence of a cDNA encoding the monkey cellular phosphoprotein p53. *Nucleic Acids Res.* **17**:8375.
- 29. Hornick, J.E., C.C. Mader, E. Tribble, C. Bagne, K.T. Vaughan, S.L. Shaw and E.H. Hinchcliffe** (2011). Amphiasmal mitotic spindle assembly in vertebrate cells lacking centrosomes. *Curr Biol.* **21**:598-605.
- 30. Durcan, T., E. Halpin, T. Rao, N. Collins, E. Tribble, J. Hornick, and E.H. Hinchcliffe.** (2008). Tektin 2 is required for central spindle microtubule organization and the completion of cytokinesis. *J Cell Biol.* **181**:595-603.
- 31. Bode, A.M., and Z. Dong** (2004). Post-translational modification of p53 in tumorigenesis. *Nat Rev Cancer* **4**:793–805.
- 32. Subramanian, R., and T.M. Kapoor** (2013). Slipping past the spindle assembly checkpoint. *Nat Cell Biol.* **15**:1261-1263.
- 33. You, Z., J.M. Balis, S.A. Johnson, S.M. Dilworth, and T. Hunter** (2007). Rapid activation of ATM on DNA flanking double-strand breaks. *Nat Cell Biol.* **9**:1311-1318.
- 34. Chen, C., L. Zhang, N-J, Huang, B. Huang, and S. Kornbluth** (2013). Suppression of DNA-damage checkpoint signaling by Rsk-mediated phosphorylation of Mre11. *Proc Natl Acad Sci USA* **110**:20605-20610.
- 35. Maze, I., K.M. Noh, A.A. Soshnev, and C.D. Allis** (2014). Every amino acid matters: essential contributions of histone variants to mammalian development and disease. *Nat Rev Genet.* **15**:259-271.
- 36. Tang, J., L.K. Qu, J. Zhang, W. Wang, J.S. Michaelson, Y.Y. Degenhardt, W.S. El-Deiry, and X. Yang** (2006). Critical role for DAXX in regulating Mdm2. *Nat Cell Biol.* **8**:855-862.
- 37. Ritchie, K., C. Seah, J. Moulin, C. Isaac, F. Dick, and N.G. Bérubé** (2008). Loss of ATRX leads to chromosome cohesion and congression defects. *J Cell Biol.* **180**:315-324.
- 38. Yang, A.H., D. Kaushal, S.K. Rehen, K. Kriedt, M.A. Kingsbury, M.J. McConnell, and J. Chun** (2003). Chromosome segregation defects contribute to aneuploidy in normal neural progenitor cells. *J Neurosci.* **23**:10454 –10462.

39. Simanshu, D.K., R. Kanth Kamlekar, D.S. Wijesinghe, X. Zou, X. Zhai, S.K. Mishra, J.G. Molotkovsky, L. Malinina, E.H. Hinchcliffe, C.E. Chalfant, R.E. Brown and D.J. Patel (2013). Non-vesicular trafficking by a ceramide-1-phosphate transfer protein regulates eicosanoids. *Nature* **500**:463-468.

40. Hinchcliffe, E. H., E. A. Thompson, F. J. Miller, J. Yang, and G. Sluder (1999). “Nucleo-cytoplasmic interactions in control of nuclear envelope breakdown and entry into mitosis in the sea urchin zygote”. *J Cell Sci.* **112**:737-746.

Figures Legends

Figure 1. Histone H3.3 Ser31 becomes phosphorylated along arms of misaligned chromosomes.

a. Prometaphase BSC1 cell treated with 2.5 μ M nocodazole for 1 Hr and stained for Aur A (green), H3.3 phospho-Ser31 (red) and chromosomes (blue). Arrowheads mark position of spindle poles. Aligned chromosomes have phospho-Ser31 at pericentromeres. Bar = 10 μ m.

b. Cell treated as in **a**, but with a single misaligned chromosome (arrow) with phospho-Ser31 along the chromosome arms.

c. Cell treated as in **a**, followed by nocodazole washout for 1 hr. Spindle poles have separated (arrows), and 3 chromosomes cluster (small arrows in inset) by the detached pole. A single misaligned chromosome is also present (arrowhead in inset). All misaligned chromosomes have phospho-Ser31 along their arms. Bar = 10 μ m.

d. Levels of phospho-Ser31 on chromosome arms as a function of number of clustered, misaligned chromosomes. Zero misaligned = all congressed. Center bar = median intensity, whiskers (error bars) = range of intensities, the maroon box = 50th percentile, and the gold box = 75th percentile.

e. Mitotic chromosomes that become isolated from other chromosomes (misaligned) trigger the genome proximity sensor. As isolated chromosomes are transported along spindle microtubules into the proximity of aligned chromosomes, the sensor is removed by a chromatin-associated phosphatase.

Figure 2. Histone H3.3 Ser31 becomes phosphorylated along arms of missegregated chromosomes in anaphase.

a. Frames from a time-lapse sequence of a mitotic BSC1- α tubulin-GFP expressing cell. At T = 2 min, the chamber was removed from the scope and chilled to 4 $^{\circ}$ C for 20 min. After the cell was returned to the scope, the depolymerized microtubules reassembled, and the cell proceeded through cytokinesis. Bar = 10 μ m. Time = Hrs:Min.

b. Increase in the

percentage of lagging chromosomes in chilled cells vs. un-treated cells. 100 anaphase cells were counted for each population. **c.** Anaphase with a lagging chromosome results in p53 stabilization. Frames from a time-lapse of a rewarmed mitotic BSC1 H2B-GFP expressing cell with a syntelic, lagging chromosome (arrows). After 4 hr, the cell had reformed both nuclei and the lagging chromosome formed a micronucleus (arrow). The cell was fixed and stained for p53 (red) and DNA (blue). Bar = 10 μ m Time = Hrs:Min. **d.** Levels of nuclear p53 in cells progressing through anaphase with lagging chromosomes vs. all congressed chromosomes. Cells were fixed at 4 hr or 24 hr post-anaphase. Center bar = median intensity, whiskers (error bars) = range of intensities, the blue box = 50th percentile, and the red box = 75th percentile. **e.** Mitotic timing for re-warmed cells that underwent anaphase with lagging chromosomes (maroon bars) vs. cells that underwent anaphase with all congressed chromosomes (gold bars). Each bar represents an individual mitotic cell, and the height of the bar represents the time from prometaphase to anaphase onset. 50 cells for each were followed. **f.** Histone H3.3 Ser31 is phosphorylated specifically on lagging chromosomes in anaphase. Frames from a time-lapse of a rewarmed mitotic BSC1 H2B-GFP expressing cell with a syntelic, lagging chromosome (arrow). As the cell progressed into anaphase, the syntelic-attached chromosome pair undergoes disjunction (arrows); it was fixed within 5 min of anaphase onset and stained for anti-Ser31P (red) and DNA (blue). **g.** Histone H3.3 Ser31 is phosphorylated on merotelic lagging chromosomes in anaphase. Another mitotic BSC1 H2B-GFP expressing cell, which congresses all chromosomes to the metaphase plate (T = 00:33), then undergoes anaphase, but contains a merotelic-attached lagging chromosome in the central spindle (small arrow). After fixation, this merotelic chromosome is preferentially phosphorylated at H3.3 Ser31. Bar = 10 μ m Time = Hrs:Min.

Figure 3. Histone H3.3 Ser31 phosphorylation spreads from individual lagging chromosomes to both nuclei following anaphase. **a.** Control cell. Frames from a time-lapse of a rewarmed mitotic BSC1 H2B-GFP expressing cell with a syntelic, lagging chromosome (arrow). Prior to disjunction, the lagging chromosome congresses, and the cell enters anaphase without lagging chromosomes. The cell was fixed ~ 1 Hr after anaphase and stained for anti-H3.3 Ser31P (red) and DNA (blue). The daughter nuclei lack H3.3 phospho-Ser31. **b.** Syntelic lagging chromosome. Frames from a time-lapse of a rewarmed mitotic BSC1 H2B-GFP expressing cell with a syntelic, lagging chromosome (arrow). The cell enters anaphase with a lagging chromosome that forms a micronucleus (arrow). The cell was fixed ~ 1 hr after anaphase and stained for anti-H3.3 Ser31P (red) and DNA (blue). Note that the micronucleus and both daughter nuclei are positive for H3.3 phospho-Ser31. **c.** Merotelic lagging chromosome. Frames from a time-lapse of a rewarmed mitotic BSC1 H2B-GFP expressing cell with all chromosomes congressed prior to anaphase onset. During anaphase a merotelic-attached chromosome pair lags in the central spindle region (arrow). These chromosomes retract to the right hand cell and form a micronucleus (arrow). The cell was fixed ~ 1 Hr after anaphase and stained for anti-H3.3 Ser31P (red) and DNA (blue). Note that the micronucleus and both daughter nuclei are positive for H3.3 phospho-Ser31. **d.** Quantitation of H3.3 phospho-Ser31 levels for cells that underwent normal anaphase (red/blue box: all chromosomes congressed) vs. cells that missegregated a chromosome during anaphase (maroon/gold box: one or more lagging chromosome). Individual mitotic BSC1 H2B-GFP expressing cells were chilled/re-warmed and followed by time-lapse as they underwent anaphase either with or without lagging chromosomes. At times indicated, they were fixed and stained for H3.3 phospho-Ser31. The Box and Whisker plot shows range, 50th and 75th percentile, as well as median values for phospho-Ser31 levels.

Figure 4. Microinjection of anti-Histone H3.3 phospho-Ser31 blocks p53 stabilization in cells that missegregate a chromosome. **a.** Control injection. Frames of a time-lapse recording of a BSC1 H2B-GFP expressing cell that was chilled/re-warmed, and then undergoes anaphase with two lagging chromosomes (arrows). At the metaphase/anaphase transition, the cell was microinjected with concentrated pre-immune IgG, followed for ~4 hr, then fixed and stained for p53 (red), DNA (blue) and rabbit IgG (green). Both daughter nuclei are positive for p53, indicating that the aneuploidy fail-safe has been activated. N = 6. **b.** Similar cell treated as described above, but injected in anaphase with concentrate anti-H3.3 phospho-Ser31. In these cells there is no stabilization of p53 in response to chromosome missegregation. **c.** Lagging chromosomes during anaphase encounter a phosphorylation gradient resulting in H3.3 Ser31 becoming phosphorylated along chromosome arms. Chromosomes that lag in the aster (syntelic) enter anaphase with phospho-Ser31, whereas chromosomes that lag in the furrow (merotelic) do not accumulate phospho-Ser31 until they become isolated from the regressing sister chromatids. In telophase, both types of cells amplify the phospho-Ser31 signal to the nascent nuclei as they reform. The result is interphase nuclei in both daughters that are phospho-Ser31, which directly leads to the stabilization and accumulation of nuclear p53.

Figure 1. Hinchcliffe et al., 2015

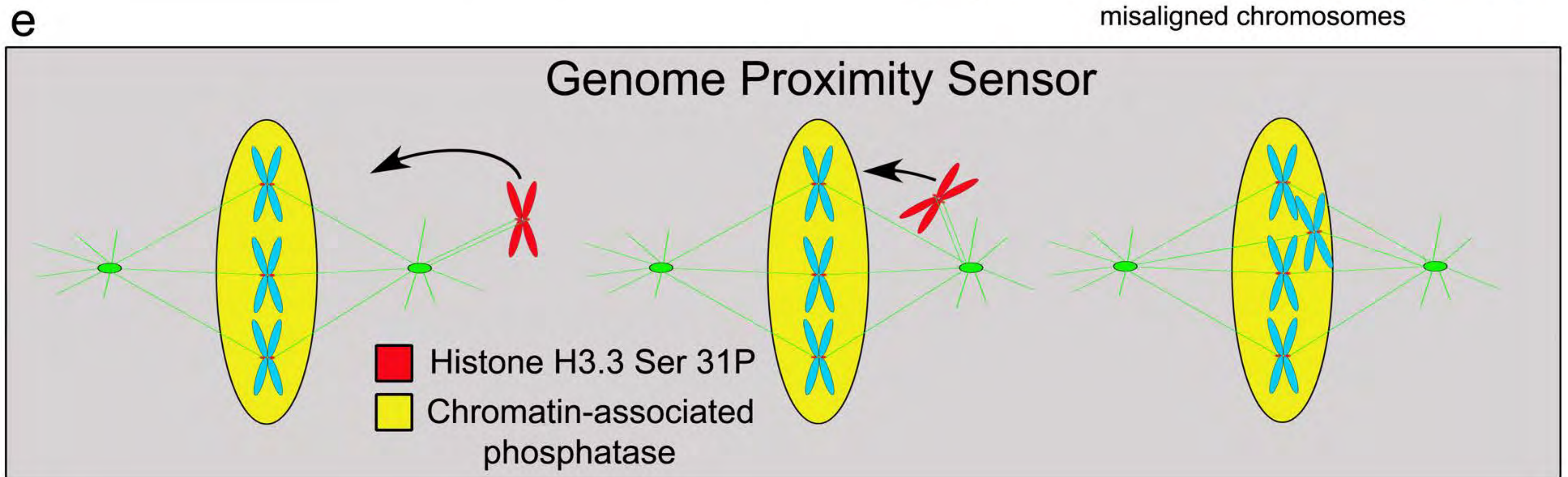
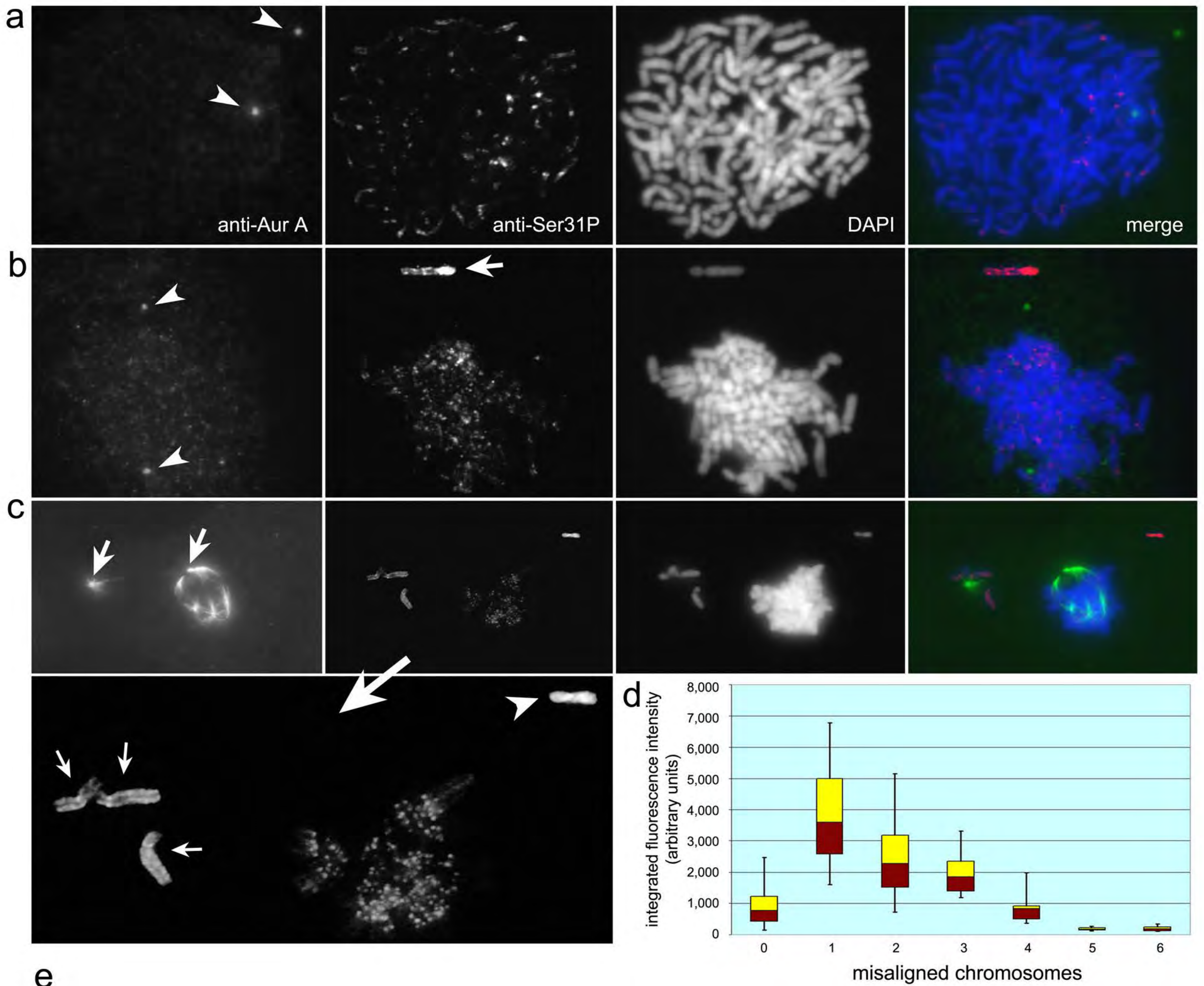
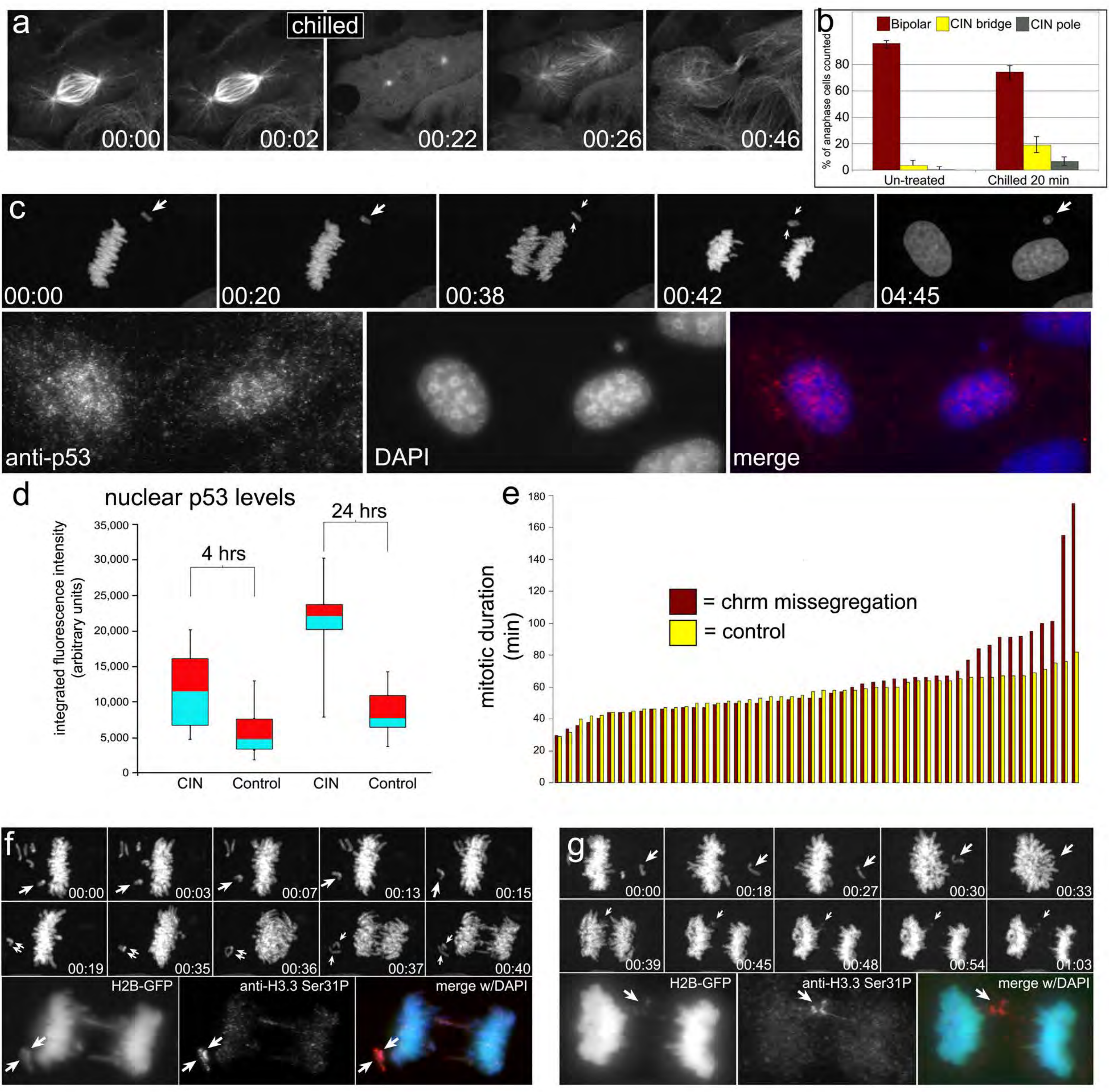


Figure 2. Hinchcliffe et al., 2015



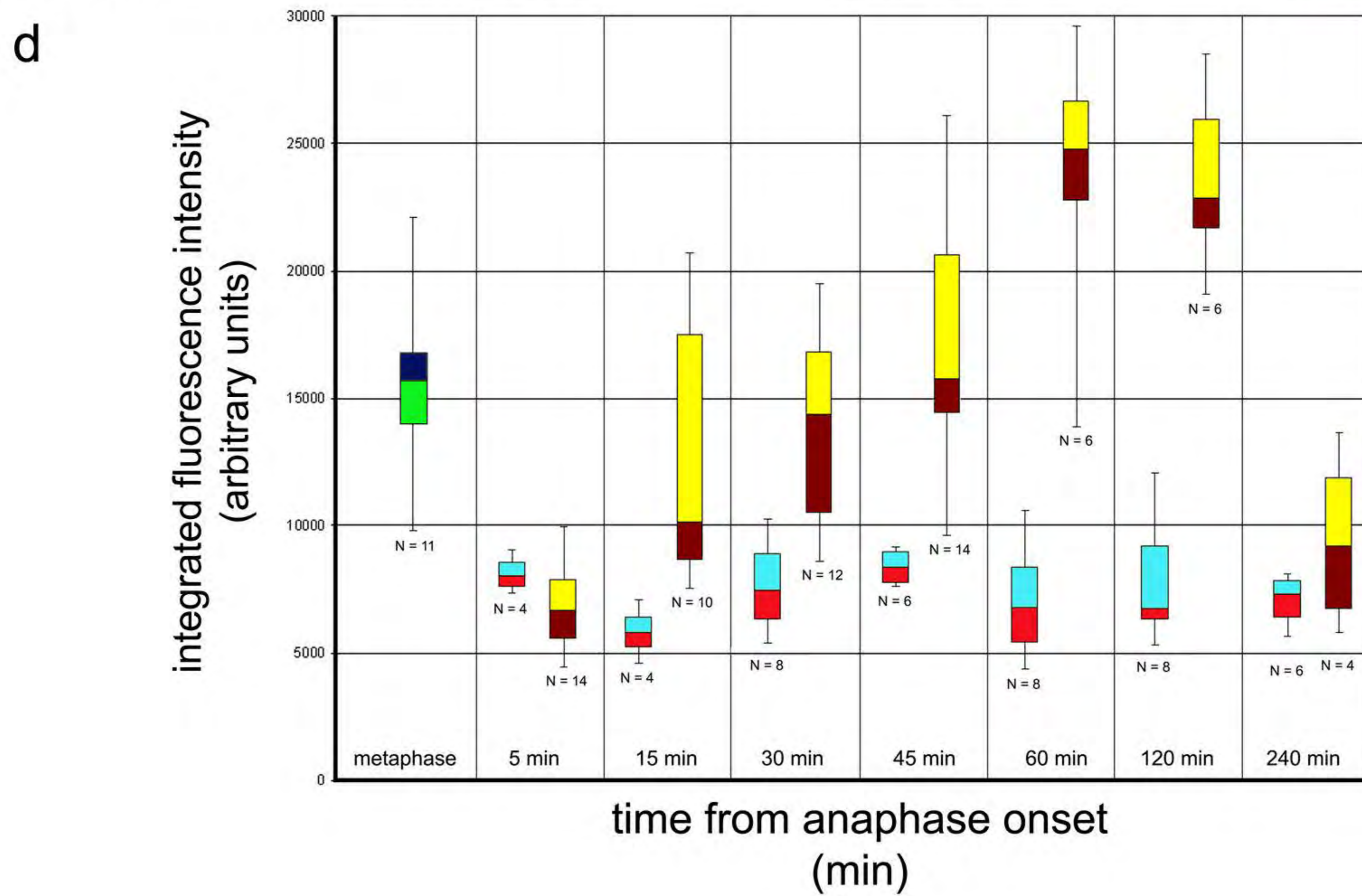
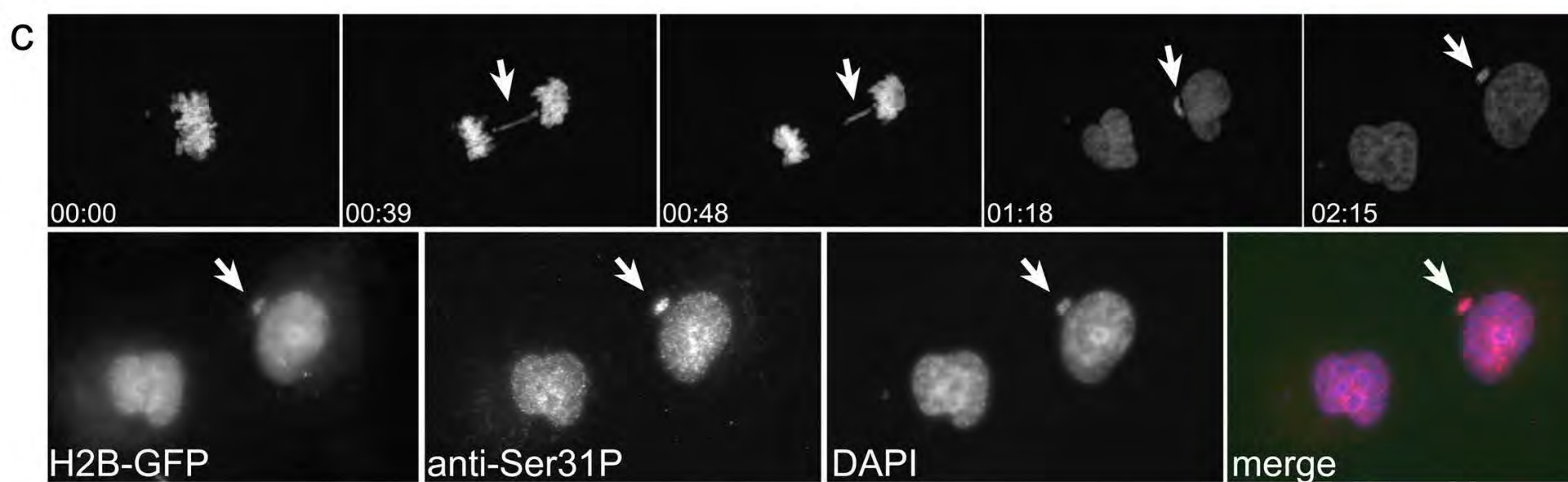
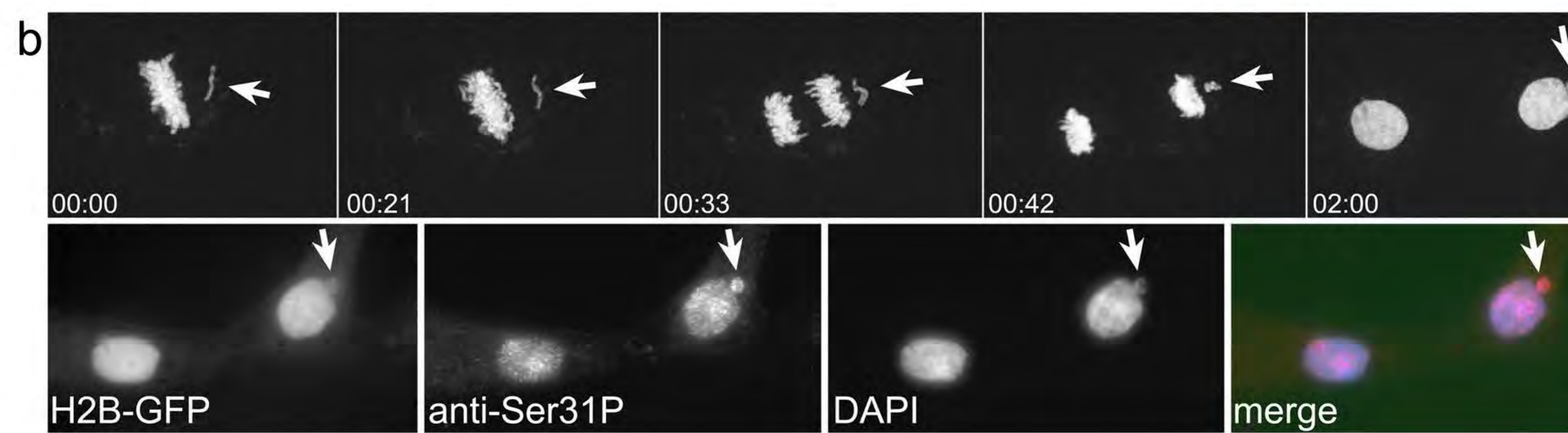
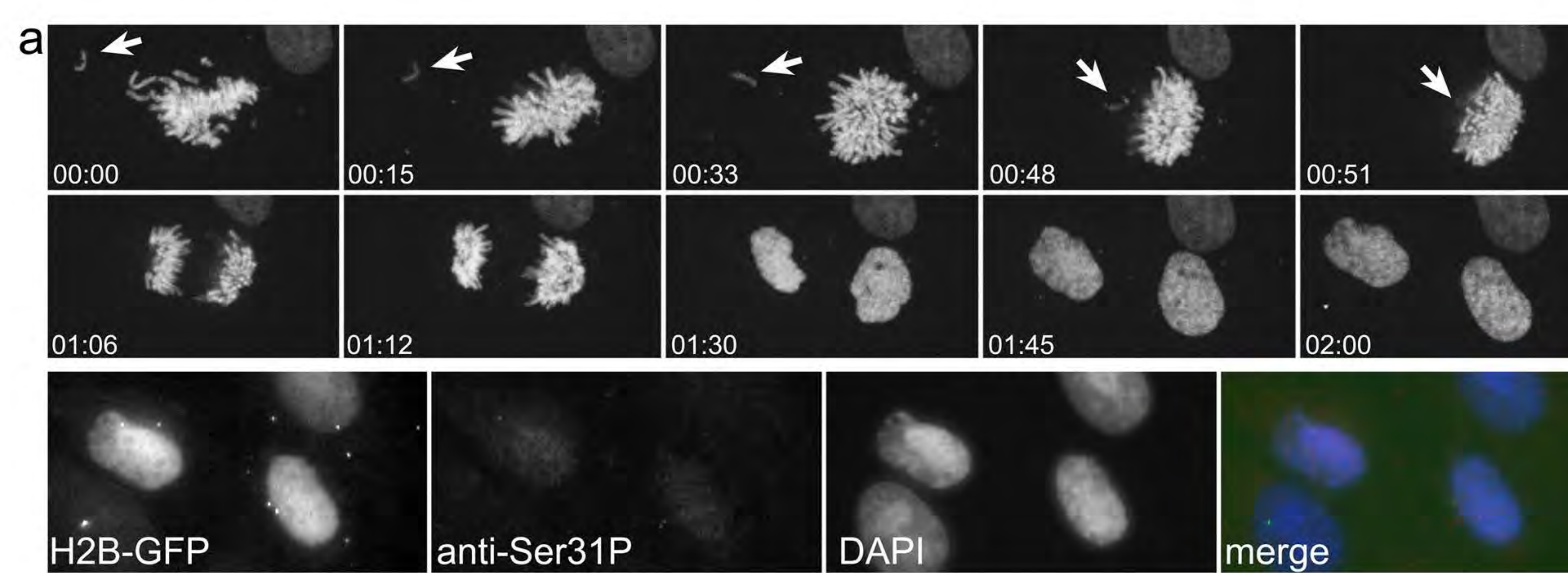
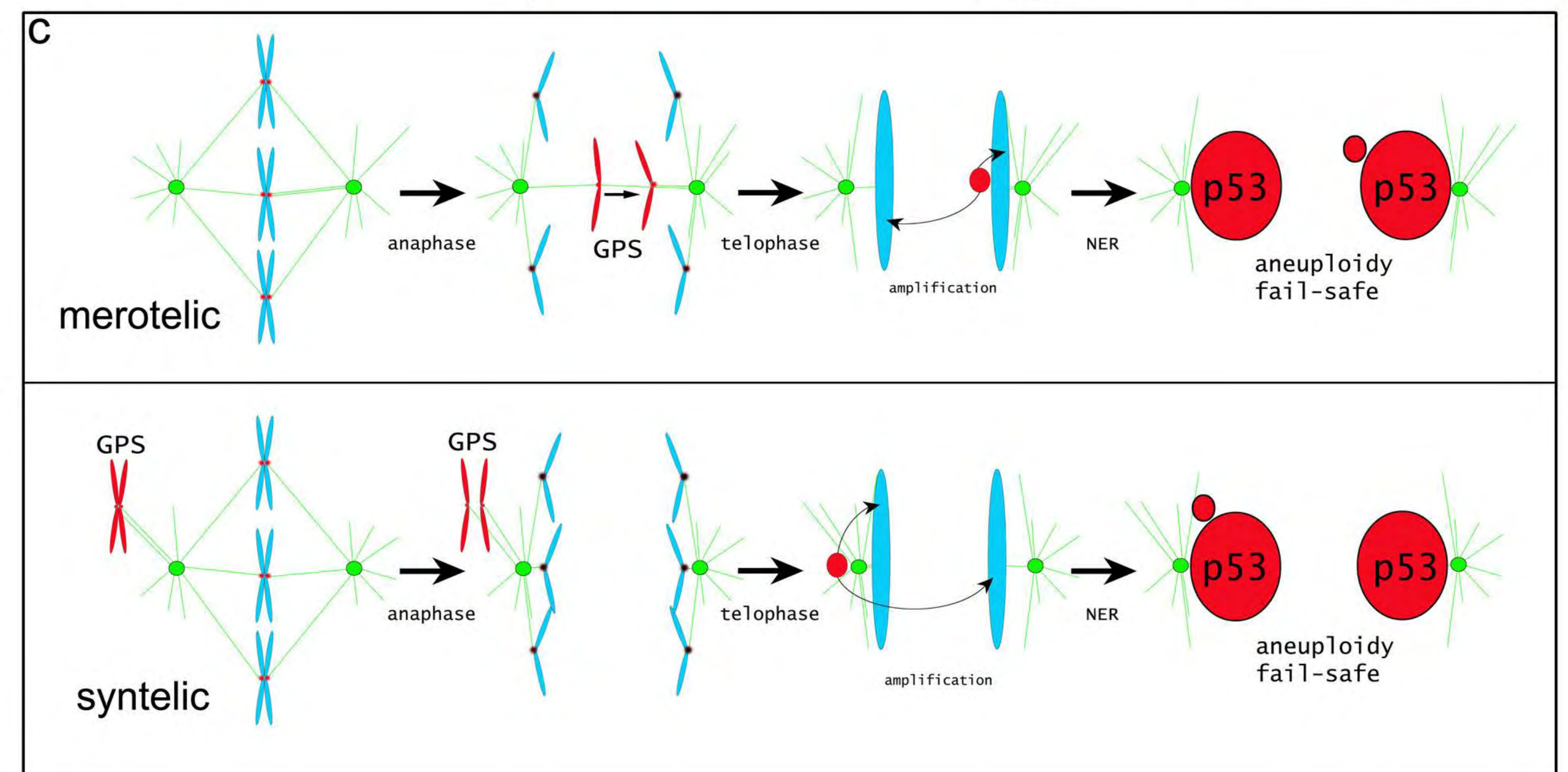
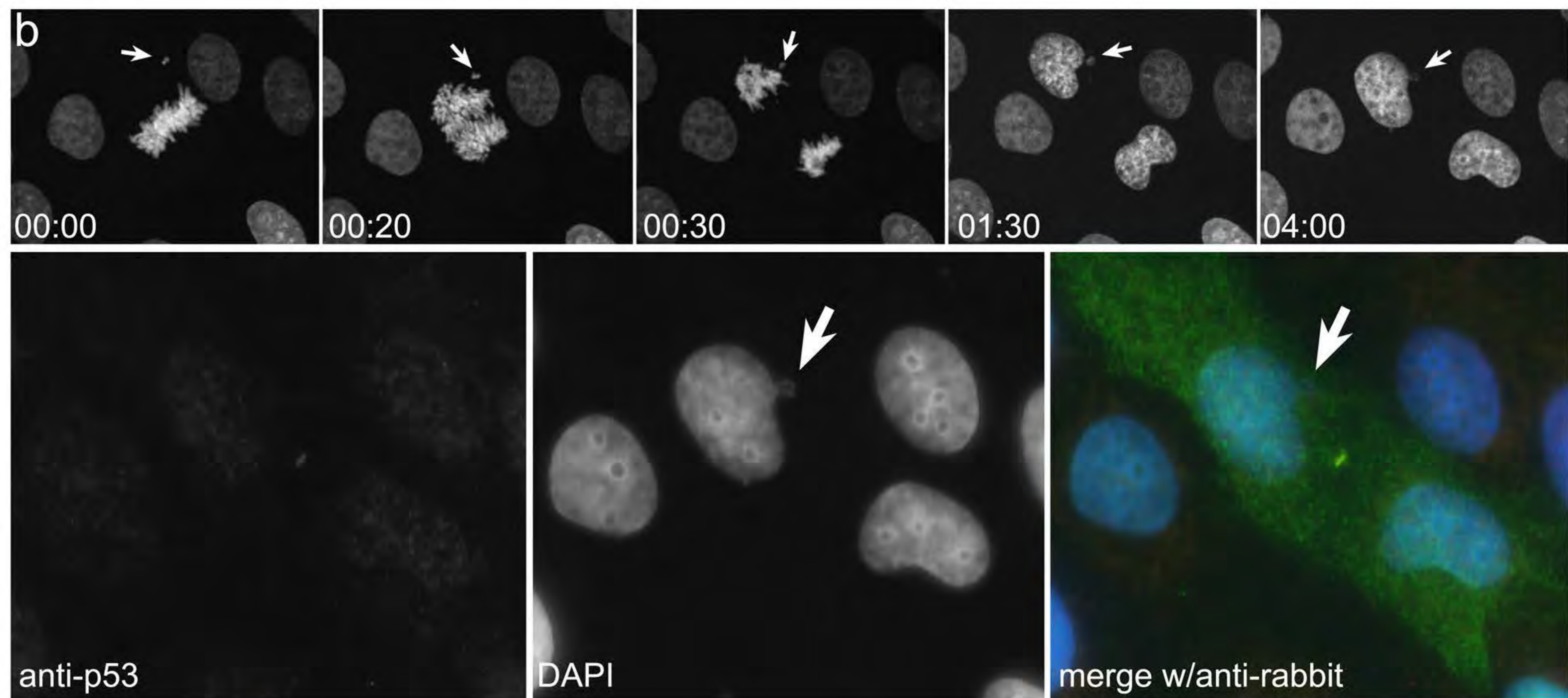
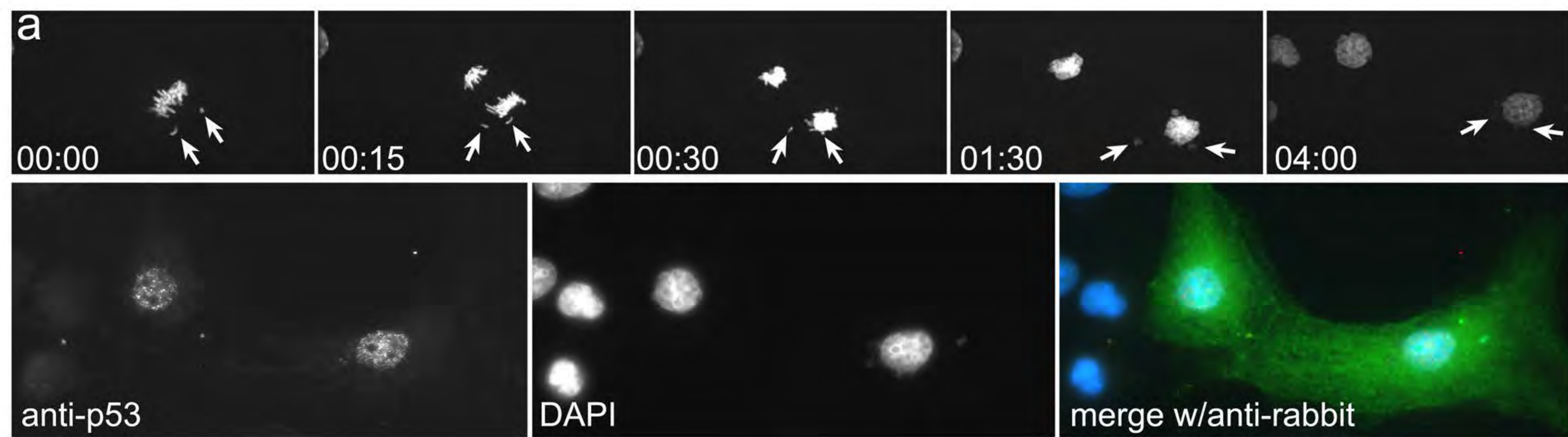
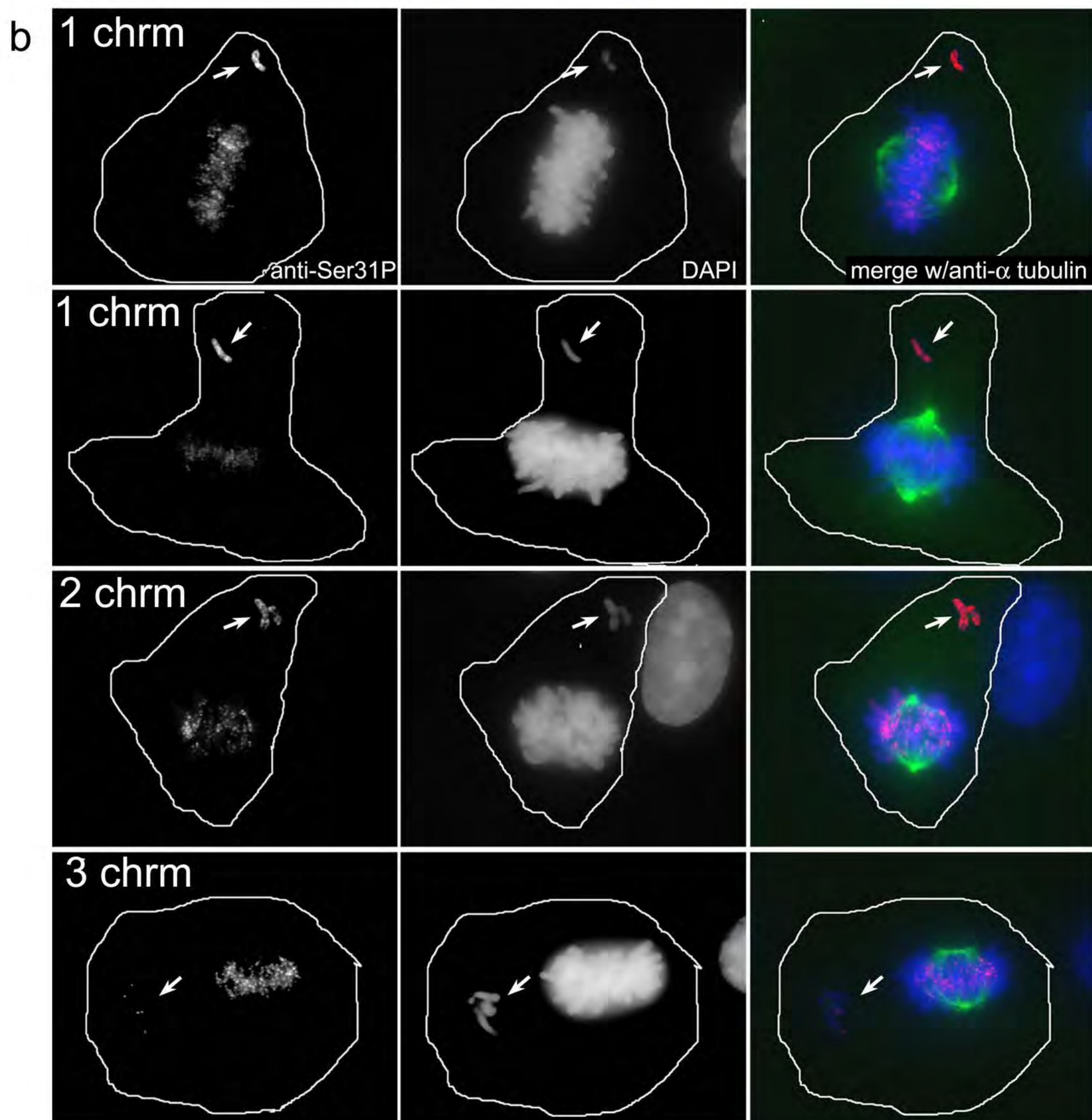
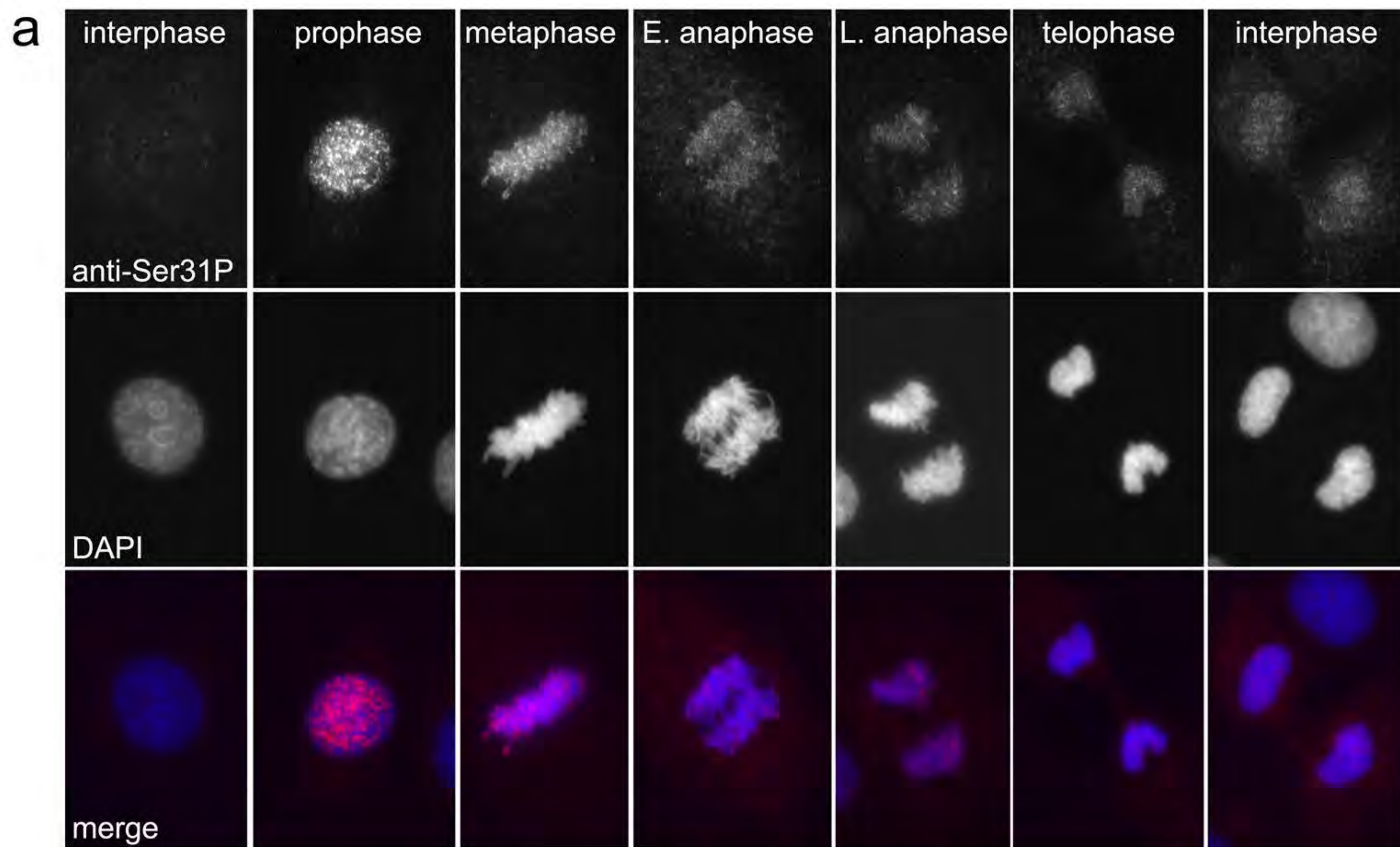
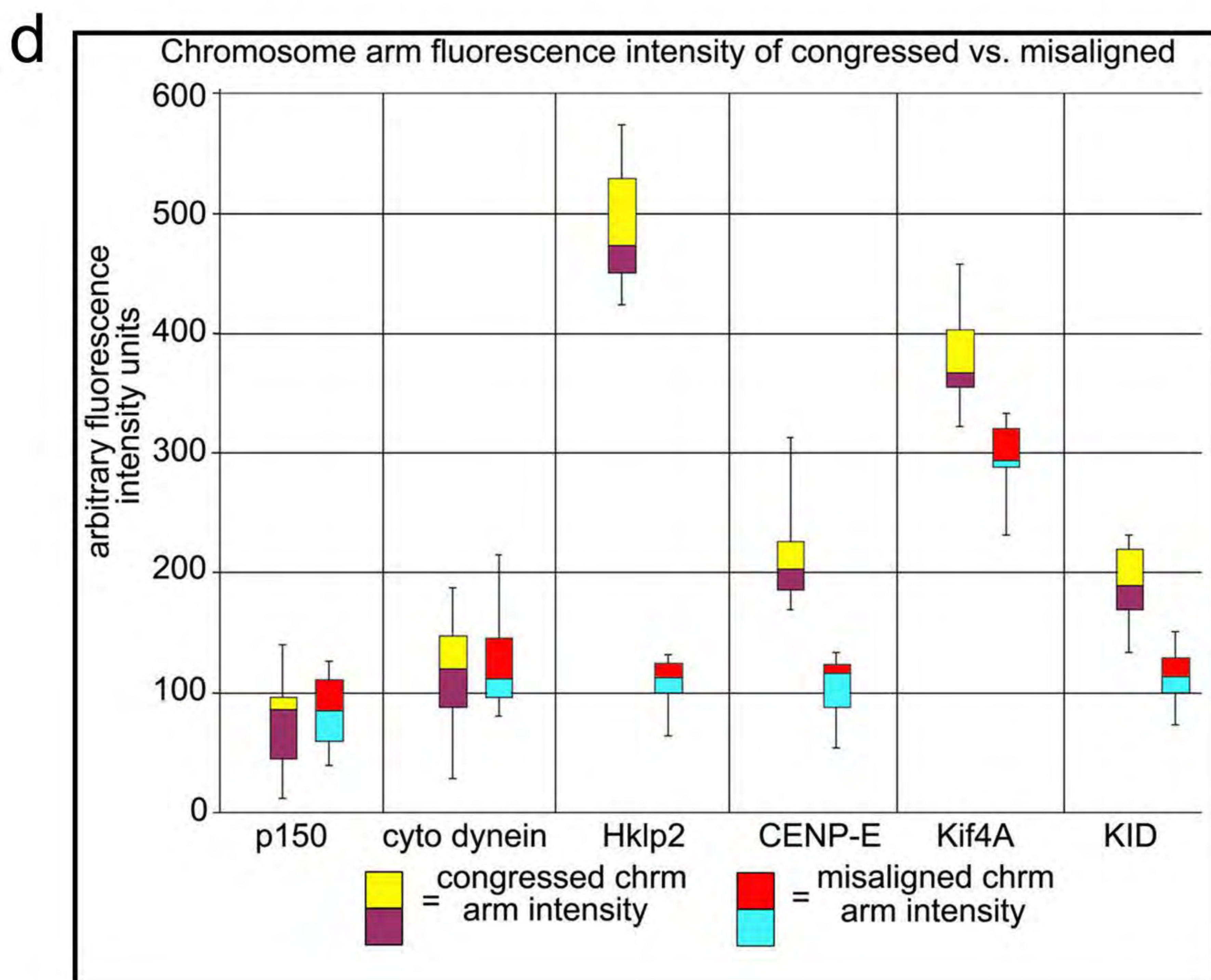
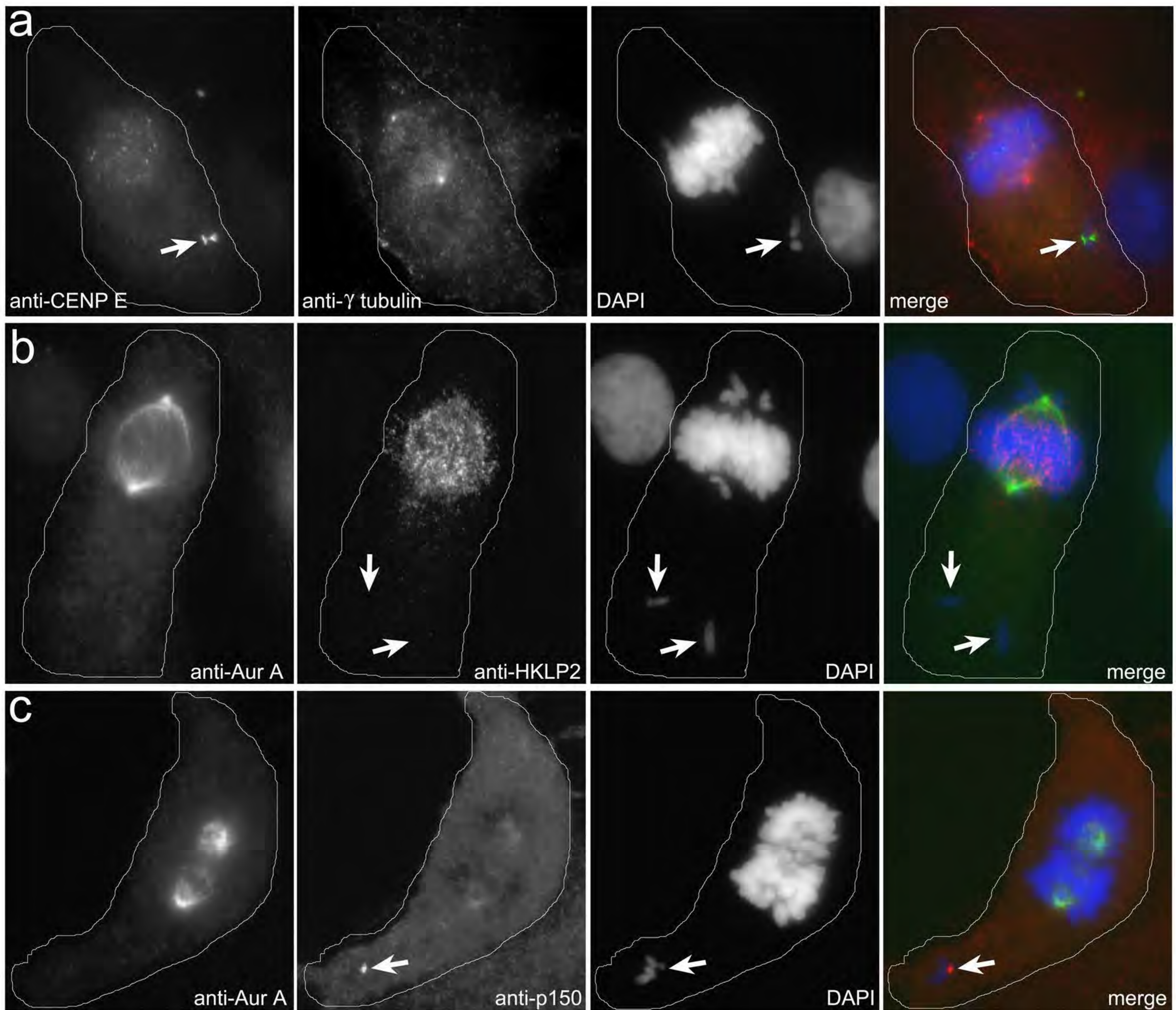


Figure 4. Hinchcliffe et al., 2015

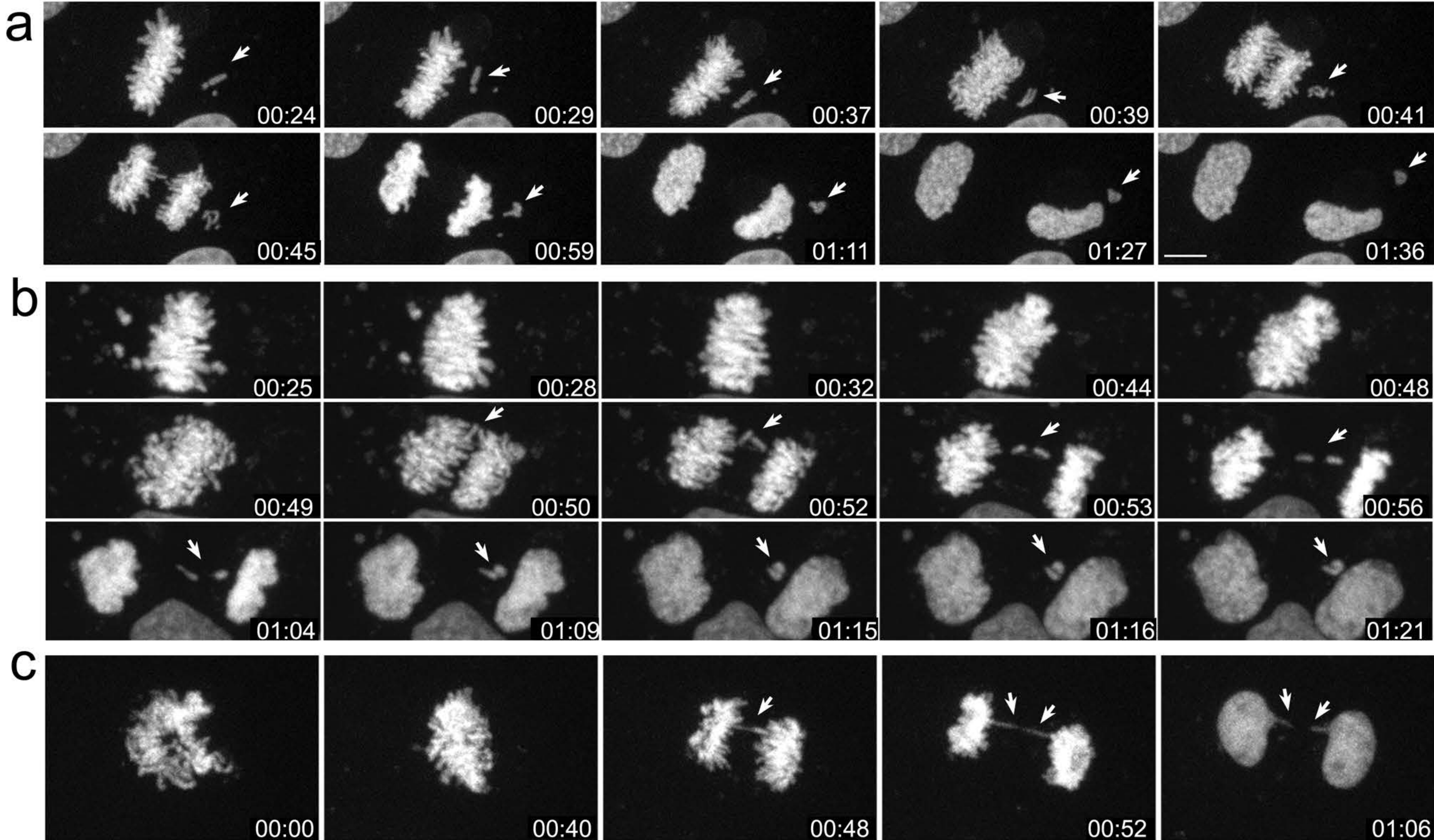


Supplemental Figure 1 Hinchcliffe et al., 2015

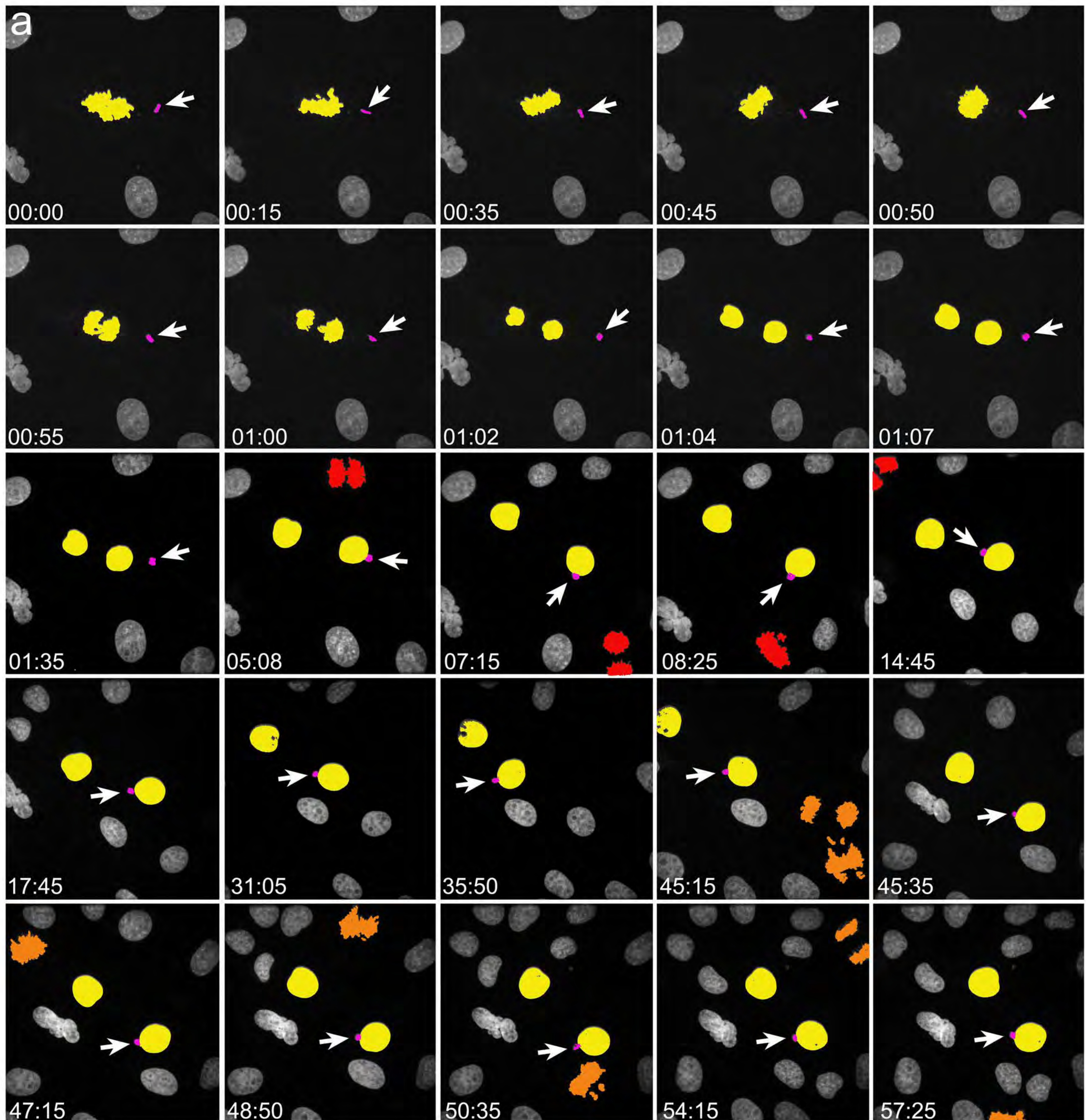




Supplemental Figure 3. Hinchcliffe et al., 2015



Supplemental Figure 4. Hinchcliffe et al., 2015



Supplemental Figure 5. Hinchcliffe et al., 2015

